NOVA SCHOOL OF SCIENCE & TECHNOLOGY

DEPARTAMENT OF MATERIALS SCIENCE

SARA ISABEL GONÇALVES PRECATADO

Bachelor of Science in Micro and Nanotechnology Engineering

OPTIMIZATION OF THE HUMAN IPS-DERIVED ENDOTHELIAL CHIP FOR DEVELOPMENT OF A 3D MICROPHYSIOLOGICAL VASCULAR CELLS SYSTEM

MASTER IN MICRO AND NANOTECHNOLOGY ENGINEERING

NOVA School of Science and Technology

April 2022

NOVA SCHOOL OF SCIENCE & TECHNOLOGY

DEPARTAMENT OF MATERIALS SCIENCE

OPTIMIZATION OF THE HUMAN IPS-DERIVED ENDOTHELIAL CHIP FOR DEVELOPMENT OF A 3D MICROPHYSIOLOGICAL VASCULAR CELLS SYSTEM

SARA ISABEL GONÇALVES PRECATADO

Bachelor of Science in Micro and Nanotechnology Engineering

Adviser: Doutor Abel Oliva, Auxiliary Researcher, Biomolecular Diagnostic Laboratory / Instituto de Tecnologia Química Biológica António Xavier

Co-adviser: Doutor Hugo Águas, Associate Professor, NOVA School of Science and Technology, NOVA University of Lisbon

Examination Committee:

Chairperson: Doutor Rui Igreja, Auxiliary Professor, NOVA School of Science and Technology, NOVA University of Lisbon

Raporteur: Doutora Raquel Barbosa Queirós, Staff Researcher, International Iberian Nanotechnology Laboratory

Members: Doutor Abel Oliva, Auxiliary Researcher, Biomolecular Diagnostic Laboratory / Instituto de Tecnologia Química Biológica António Xavier

MASTER IN MICRO AND NANOTECHNOLOGY ENGINEERING

NOVA School of Science and Technology
April 2022

Optimization of the human iPS-derived endothelial chip for development of a 3D microphysiological vascular cells system

Acknowledgements

The delivery of this dissertation marks the end of this stage of my life, the culmination of 18 years of studying. I am very grateful to all the people who direct or indirectly supported me throughout these 6 years of college and especially throughout the last year.

First of all, I have to express my gratitude to my adviser Doutor Abel Oliva, my co-adviser Doutor Hugo Águas and to Doutor José Belo and Doutor José Inácio for giving me the opportunity of contributing to this project. To Doutor Abel Oliva for having welcomed me into his research group at Instituto Tecnologia Química e Biológica, for all the support and helpful ideas, for the trust placed in me, for allowing me to grow and for always instilling in me the spirit of resilience when things did not go as expected. To Doutor Hugo Águas for all the teachings over these years, for having awakened my curiosity about microfluidics and for always being available at the distance of an email or a video call. To Doutor José Belo and Doutor José Inácio, for having welcomed me into them research group at Chronic Diseases Research Centre, for the availability, support and teachings given during the biological work in the last few months.

To my faculty, NOVA School of Science and Technology (FCT NOVA) for allowing me to study in one of the most recent and scientifically advanced areas – nanotechnology. To the institutions that have made this work possible – Instituto Tecnologia Química e Biológica (ITQB), Centre of Excellence in Microelectronics Optoelectronics and Processes (CEMOP) and Chronic Diseases Research Centre (CEDOC) – for always providing the necessary resources and the cooperation shown.

To the Biomolecular Diagnosis Group at ITQB, who received me with kindness and for always being available. To Sara, Mafalda and Rafaela for all the guidance given, for answering all my questions and for the company during lunchtime. To Dragana for all the company in the laboratory and for always having a friendly word at the end of the day.

To Stem Cells and Development Laboratory at CEDOC, who received me during the last months of this thesis and for happily sharing with me your work and being interested in mine even though we have different backgrounds.

I would like to thank Marta Magalhães, who preceded me in the work of the master's thesis, for introducing me to her work, for her tips on what to improve and for always being available to answer my questions about the protocols.

This work would not be possible without all the people that collaborated on it. To André Moura and José Fernandes for all the help, patience and availability for guiding me with the processes of microfabrication in the cleanroom and to Sara Baptista for the availability to print me all the 3D pieces that I required.

To all my friends, inside and outside college, a huge thank you for being part of my life and for always asking if my cells were alive. To my best friends Mariana, Guerra and Francisca for always being by my side, for all the love and friendship and for always supporting and cheering me up. Those that Chemical and Biochemical Engineering brought me, Sara and Bia, you were with me from the first week of college and I can't wait to see what life brings us. To my Micro and Nano friends, Andreia, Beatriz and Marta, for welcoming me on a strange course and for the friendship and companionship during these years. To all my freshmen, thank you for making me feel that I have a family in Nano.

To my boyfriend, Tomás, for the unconditional support, love and friendship that showed me every year together. For always showing me the positive side of life, for encouraging me to achieve everything I desire and for never leaving my side. Without you, it would never be as easy as it was.

Lastly but not least, to my family a huge thank you for the unconditional love, support and constant belief in me. For always encouraging me to be the best person I can be and supporting me through all my decisions. For always counselling me, helping me find answers to every question I had and for always being there for me.

"Science, my lad, is made up of mistakes,
but they are mistakes which it is useful to make,
because they lead little by little to the truth."

Julio Verne

Abstract

This work aimed to obtain an interconnected vascular network of endothelial cells within a microfluidic device. For this, two layouts of microfluidic devices were designed, fabricated in polydimethylsiloxane (PDMS) through photo and soft-lithography techniques and co-cultured with human umbilical vein endothelial cells (HUVECs) and fibroblasts as support. To promote uniform cell growth inside the tissue chambers of the chip, an oscillating culture media delivery system was optimized to create a pressure gradient by maintaining a difference in level between two culture media containers. The system was operated by a servo motor connected to a microcontroller board and automatically oscillated the positions of the culture media containers every 24 hours. The culture media flow and the time between the oscillating movements could be defined before each assay in the OLED menu. Several assays with different concentrations of fibroblasts were carried out to evaluate the optimization of cell seeding and culture media protocols. The results revealed that the growth of cellular networks is inversely related to the concentration of cells. The lower the concentration of fibroblasts seeded in the chip, the longer it takes for their growth. After the optimization of the assays protocols, different concentrations of fibroblasts and HUVECs were combined with fibrin-thrombin hydrogel and seeded into the chips. As a result, it was possible to observe after 14 days signs of cell growth mimicking an interconnected network of blood vessels, indicating that this optimized platform has the potential to develop a 3D vascular network when co-culture with endothelial cells and fibroblasts.

Keywords: Organ-on-a-chip, Vasculature-on-a-chip, Microfluidics, PDMS, Fibroblasts, Endothelial Cells

Resumo

Este trabalho tem como objetivo obter uma rede vascular de células endoteliais num dispositivo de microfluídica. Para isso, foram desenhados dois modelos de chips de microfluídica, fabricados em dimetilpolissiloxano (PDMS) através de técnicas de fotolitografia e litrografia suave e semeados com células endoteliais de veia umbilical humana (HUVECs) e fibroblastos como suporte. Para promover um crescimento uniforme de células dentro das câmaras do chip, foi otimizado um sistema oscilante de entrega de meio de cultura de modo a criar um gradiente de pressão devido a uma diferença de nível entre os recipientes com o meio. O sistema foi operado por um servomotor conectado a um microcontrolador oscilando automaticamente as posições dos recipientes dos meios de cultura a cada 24 horas. O fluxo do meio de cultura e o tempo entre os movimentos oscilantes podiam ser definidos antes de cada ensaio no menu OLED. Vários ensaios com diferentes concentrações de fibroblastos foram realizados para avaliar a otimização dos protocolos de introdução de células e do meio de cultura no chip. Os resultados revelaram que o crescimento das redes celulares está inversamente relacionado com a concentração de células. Quanto menor a concentração de fibroblastos semeados no chip, mais tempo leva para o seu crescimento. Após a otimização dos protocolos, diferentes concentrações combinadas de fibroblastos e HUVECs foram adicionadas a um hidrogel de fibrina-trombina e semeadas nos chips. Como resultado, após 14 dias, foi possível observar sinais de crescimento celular mimetizando uma rede interconectada de vasos sanguíneos, indicando que esta plataforma otimizada tem potencial para desenvolver uma rede vascular 3D quando semeada com células endoteliais e fibroblastos.

Palavras-chave: Organ-on-a-chip, Vasculature-on-a-chip, Microfluídica, PDMS, Fibroblastos, Células Endoteliais

Table of Content

List of Figures

List of Tables

Acronyms

BS	Blocking Solution
CCBE1	Collagen and Calcium-Binding Epidermal Growth Factor domain-1
CEDOC/NMS	Chronic Diseases Research Center / NOVA Medical School
CVDs	Cardiovascular Diseases
DAPI	4',6-diamidino-2-phenylindole
DMEM	Dulbecco's Modified Eagle's Medium
ECs	Endothelial Cells
ECM	Extracellular Matrix
EDTA	Ethylenediaminetetraacetic Acid
EGM-2	Endothelial Cell Growth Medium-2
FBS	Fetal Bovine Serum
HDFn	Human Dermal Fibroblasts, neonatal
HUVECs	Human Umbilical Vein Endothelial Cells
IPA	Isopropyl Alcohol
iPSCs	Induced Pluripotent Stem Cells
iPS-ECs	Induced Pluripotent Stem Cell-Derived Endothelial Cells
MEFs	Mouse Embryonic Fibroblasts
OLED	Organic Light-Emitting Diode
OoC	Organ-on-a-Chip
PBS	Phosphate-Buffered Saline
PDMS	Polydimethylsiloxane
PFA	Paraformaldehyde
PFOCTS	Trichloro(1H,1H,2H,2H-perfluorooctyl)silane
PGMEA	Propylene Glycol Methyl Ether Acetate
PLA	Polylactic Acid
PMMA	Polymethyl Methacrylate
PS	Penicillin-Streptomycin
RIE – ICP	Reactive Ion Etching – Inductively Coupled Plasma
T175	175 cm^2 Surface Area T-flask

UV	Ultraviolet
VEGF	Vascular Endothelial Growth Factor

Symbols

C_f	Final Concentration
C_i	Initial Concentration
V_{cells}	Volume of Cells
V_f	Final Volume
V_i	Initial Volume
$V_{trypan\ blue}$	Volume of Trypan Blue Solution

1. Motivation and Objectives

According to the World Health Organization, cardiovascular diseases (CVDs) have become the main cause of death globally (37%) and are responsible for an estimated 17.9 million deaths in 2019 [1]. CVDs are a group of disorders in the cardiovascular system, including stroke, coronary heart disease, cerebrovascular disease, congenital heart disease, vein thrombosis and pulmonary embolism. In the cardiovascular system, the blood is pumped by the heart through the vasculature. A malfunction of these components, aligned with hereditarian susceptibility can lead to a wide range of cardiovascular system disorders symptoms. Due to the high mortality, there is a need for CVDs researchers to study the physiological and pathological mechanisms, develop diagnostic methods and therapeutic treatments [2].

In this way, microfluidics - specially Organ-on-a-Chip (OoC) devices - are a technology that can be used to investigate all three aspects of CVDs research. The main goal of this thesis was to obtain a platform capable of forming a network of differentiated endothelial cells originated from induced pluripotent stem cell-derived endothelial cells (iPS-ECs), with physiological functions that respond to shear stress, with perfusion vascular networks within a 3D microfluidic device. To achieve this goal, several objectives were defined as follows:

- Optimization of the previous designs of the microfluidic devices, taking into account the aspects to be improved;
- Fabrication through photo and soft-lithography techniques of numerous microfluidic devices;
- Optimization of the automatic oscillator culture media feeding platform;
- Optimization of the assay protocols, including sterility procedures, cell culture, and growing media handling;
- Pre-testing the developed platforms with fibroblasts cells;
- Co-culturing endothelial cells and fibroblasts into the microfluidic devices.

2. Introduction

2.1 Microfluidics

Microfluidics in microengineering emerges as a science that studies the behaviour, control, and manipulation of microscale fluids (10^{-9} to 10^{-18} L) through microchannels with at least one dimension of 1 to 100 μm [3], [4]. Formerly introduced by the microelectronic industry, the applications for this technology currently integrate fields of biology, chemistry, energy, and biomedicine [5]. The development of Lab-on-a-Chip devices brought forward the microfluidics research since it appears they can integrate an entire biological or chemical laboratory into a single chip performing analysis in an automated routine. [6], [7]. This technology lead to the appearance of OoC devices which was an important breakthrough for medicine and biology since it narrows the differences between *in vitro* and *in vivo* models [8].

Microfluidic devices provide several benefits over conventional sized chemical and biological systems. The small volume of the sample and reagents required, since it is on a microscale, results in the possibility to process and analyse limited expensive and/or hazardous samples with minor sample handling [6]. Moreover, it is possible to carry out detection with high resolution and sensitivity considering that there is a decrease in sample loss and dilution as well as customized architecture design of the chip. The small sizes associated with this technology result in faster response times, along with better efficacity in integrating microfluidic components for simultaneous processing [7], [9].

Microfluidic devices can be made with different materials according to their application. Silicon has been used in microfluidic devices since is resistant to organic solvents and has high thermal conductivity, however, its opacity limits the imaging and detection process in the visible and ultraviolet regions and it is a relatively expensive and fragile material [4], [10]. Glass could overcome the opacity problem since it has excellent optical transparency; however, it has high fabrication cost and long processing times [5], [10]. All these limitations instigate the development of alternative transparent or semitransparent low-cost chip materials that can be easily fabricated as polymers.

One of the most common polymers used for microfluidic devices is polydimethylsiloxane (PDMS), a silicon-based synthetic polymer that has the advantage of being biocompatible, optically clear, thermally stable, highly flexible, having high oxygen permeability and reduced fabrication cost [8]. However, because of its porosity, is it incompatible with organic solvents as their molecules can be adsorbed [5], [10].

Thermoplastics such as polystyrene, polymethyl methacrylate (PMMA) and polycarbonate are other examples of polymers that can be used. These materials can provide the microfluidic device with mechanical stability pursuing a high resistance to pressure and temperature fluctuations due to their stable surface chemistries. However, they can be non-transparent and are not suitable for long-term cell cultures since they have poor gas permeability [5], [12].

2.2 Organ-on-a-Chip.

Drug development is slow and costly mainly due to the *in vivo* animal preclinical studies limitations. In addition, the accuracy and reproducibility of the testing results obtained from animal studies do not always translate the expected therapeutic effect in the human body due to differences between the animal and human physiological systems [13], [14]. The Biotechnology Innovation Organization concluded that approximately 70% of newly developed drugs fail in human clinical trials even though they accomplished preclinical evaluation, including animal tests [15].

Therefore, alternative tissue models that could replicate the human pathophysiology were required. The OoC is described as a microfluidic cell culture device that can mimic the complex environment of a physiological human organ in a controlled manner [5], [12]. By creating chambers and microchannels compatible with cell culturing with the silicon-based polymer PDMS, and supported by flowing reagents and culture media, it is possible to control the movement and behaviour of cells to imitate the physiological and mechanical conditions of a specific organ.

As a result of the need for accurate human organs models in the medical field, there were emerging different types of single-organ chips including, for example, Liver-on-chip, Lungs-on-chip, Kidney-on-chip [3], and more specifically for CVDs research, Heart-on-chip [3], and Vasculature-on-Chip [16]. These devices have been successfully developed for analyzing adverse drug reactions as well as investigating disease progression.

2.2.1 Vasculature-on-a-Chip

The vasculature is the main structure of the circulatory system responsible for transporting oxygen, nutrients and biological secretions through the human body and for homeostasis maintenance [17]. It differentiates into three complex structures: the arterial section with arteries and arterioles; the venous section with veins and venules and the capillaries. Despite the differences between these complex structures, which are adjusted to fulfil their functions, the entire vasculature is lined inside by endothelial cells (ECs) [18], [19].

ECs form a polarized monolayer with their luminal membrane exposed to blood constituents and circulating cells and their basolateral surface facing the vascular matrix, being aligned to the blood vessel axel to minimize the shear stress applied by the circulating blood [20]. ECs are generally thin and elongated despite displaying considerable heterogeneity in structure (cellular morphology) and function across the different regions of the body [20], [21]. They form a tissue-type dependent permeable barrier for the blood vessel, which performed some physiological functions such as blood vessel formation and regression, regulation of the blood flow and hemostatic balance [17].

In vivo, a dysfunction or dysregulation of the blood vessels can lead to a multitude of pathologies such as atherosclerosis, cancer metastasis and tumour angiogenesis [18]. Experimental vascular network models, namely Vasculature-on-Chip (Figure 2.1), have been progressively investigated in the last decade since there are of great importance for understanding the mechanisms of vascular diseases promoting future developments of diagnostic or therapeutic strategies [22].

Before attempting to recreate an *in vitro* vasculature, it is essential to understand the biological processes of the *in vivo* vasculature. During the formation of vessels, a process called vasculogenesis occurs mostly during embryonic development, in which it differentiates angioblasts (endothelial precursor cells) into ECs to form an arterial or venous capillary vessel. Angiogenesis follows vasculogenesis, to remodel and expand the circulatory system during a physiological condition (embryonic development or a wound healing process) and/or a pathological condition (tumour growth) by creating a new vasculature arrangement from a pre-existing vessel

[19][23]. Previous studies have shown that fibroblasts have a critical role in this process through the extracellular matrix (ECM) synthesis and maintenance, and growth factors secretion that promotes the ECs proliferation and adhesion to the ECM [23], [24]. Therefore, to try to mimic the *in vivo* environment and reproduce the angiogenic process *in vitro*, human ECs have to be co-cultured with fibroblasts, their usual partner in connective tissues.

Bonet et al [25] proved that the collagen and calcium-binding epidermal growth factor domain-1 protein (CCBE1) is an extracellular matrix protein essential for coronary vessels development. CCBE1 is a protein code gene that is required for angiogenic sprouting from the venous endothelium during embryogenesis. In the CCBE1–deficient mice the coronary vessels were underdeveloped compared to the same vessels in wild-type hearts.

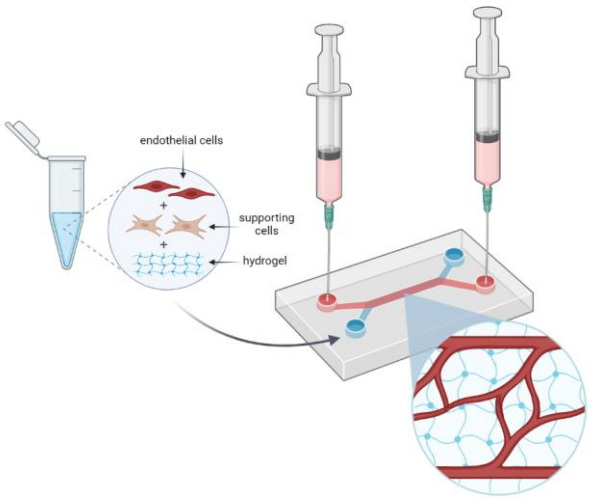

Figure 2.1 – Schematic representation of a vasculature-on-a-chip [Figure created with Biorender.com].

2.2.1.1 Hydrogel-based Microfluidics

A typical approach to recreating the intricate vasculature *in vitro* is by using 3D hydrogel inside the microfluidic device. Hydrogels are extremely porous three-dimensional network structures of hydrophilic polymers that are capable of small molecules diffusion and resemble the ECM [10]. Because of their characteristics, they are ideal to assist cell organization by providing a similar *in vivo* physiological environment [22]. In that way, co-culturing ECs with other types of cells, e.g. fibroblasts in a soft hydrogel, permits the construction of a 3D matrix for the development of vascular cells. For example, Kurokawa et al. [26] engineered perfusable vascular networks into Matrigel (a solubilized ECM membrane matrix extracted from Engelbreth–Holm–Swarm mouse sarcoma cells produced by Corning Life Sciences) and Kim et al. [27] demonstrated the formation of a perfusable and functional endothelialized microvascular network in fibrin with human umbilical vein endothelial cells (HUVECs) and fibroblasts.

There are several examples of hydrogels widely used in tissue engineering that can encapsulate cells including type I collagen [28], Matrigel [26], alginate [29] and fibrin [30][31]. Fibrin is an insoluble fibrous protein involved in the blood clotting process and is formed by the polymerization of fibrinogen, a soluble macromolecule, initiated by protease thrombin. By forming an insoluble clot, fibrin is essential to hemostasis and wound healing [32] and due to its characteristics has been selected to be used in this work.

2.2.1.2 Induced Pluripotent Stem Cell-Derived Endothelial Cells

While significant efforts have been made to create vascularized tissues, most reports use primary endothelial cells [27], [30]. However, due to their limited availability and ethical controversy associated with the use of human embryonic stem cells [33], there has been a growing interest in endothelial cells derived from human induced pluripotent stem cells (iPS-ECs) to create vessel networks [17]. Takahashi et al. discovered induced pluripotent stem cells (iPSCs) over a decade ago [34] for which the Nobel Prize was awarded in 2012. Nowadays they represent a source of vascular and other cells, without the problems associated with primary endothelial cells because they can be derived by reprogramming somatic cells from any individual, increasing their availability [17].

A wide variety of human tissues can be generated from iPSCs. Human iPSCs are a valuable source of vascular cells since they reproduce the individuals' genetic background from whom derived. However, to obtain a phenotypically pure cell type, the isolation and cell differentiation methods require extremely complex skills, are expensive and time-consuming [35].

In 2018, the functionality of iPS-ECs was compared with primary ECs [36]. This study showed that barrier function and inflammatory responses were consistent in different iPS-ECs lines of cells and when compared to HUVECs showed a higher barrier function and lower inflammatory responses.

In vitro models based on iPS-ECs cultured in microfluidic chips are now being reported. Kurokawa et al. [26] used human iPS-ECs cultured in a custom hydrogel inside a microfluidic device and generated a 3D perfusable capillary network that was stable for at least 14 days. The cells demonstrated physiological functions of endothelial cells, displayed a predominantly venous phenotype and responded to shear stress. More recent, Vila Cuenca et al. [31] developed a 3D vessel-on-a-chip model with human iPS-ECs and human iPSC-derived vascular smooth muscle cells in a fibrin hydrogel microenvironment. They demonstrated the formation of an interconnected microvascular network by iPS-ECs and better ECs self-organization and vessel stability by the presence of mural cells. Mural cells surround the endothelium and are important components of the microvessels considering their critical role in vasculature growth and maturation, regulation of blood pressure and maintenance of vessel stability [37].

2.3 Fabrication Methods

Microfabrication consists of devices fabrication to a micrometre scale or smaller. To achieve a perfusable microvascular model is require the creation of perfused microchannels within a polymer substrate and two different approaches can be used. The first fabrication approach is “bottom-up” where the ECs are seeded into hydrogels, with or without stromal cells such as fibroblasts, to develop vascular networks, without the requirement of microstructure. However, the heterogeneity of vascular size, length, and geometry can result in uncontrollable flow patterns so the second and more popular approach is the “top-down” approach. In this method, the microstructures are fabricated before seeding the cells [38].

Within “top-down” approaches, there are a variety of fabrication techniques being used including 3D printing, injection moulding and photolithography and soft-lithography, the latter being used in this work. 3D printing consists of a layer-by-layer method where sacrificial templates are printed onto a matrix and subsequently removed resulting in organized microchannels formation [10]. For instance, Nie et al. [39] printed hydrogel-based chips with channels of diverse forms and demonstrated the formation of lumen structures by seeding HUVECs in collagen-treated channels, indicating the vascularization of the channels. Injection moulding is a common technique where the thermoplastic melted is injected under pressure into the pre-compressed heated

mould cavity and later removed. Ko et al. [40] presented an injected 3D vascular network platform to study angiogenesis by patterning HUVECs and lung fibroblasts.

The most common techniques for OoCs fabrication are photolithography and soft-lithography [26], [27], [29], [30], [41], in which negative photoresists (photosensitive polymers) are generally spin-coated on top of a silicon wafer. SU-8 is the most used negative photoresist since it provides a wide range of layer thickness depending on its viscosity. The SU-8 film deposited is then patterned by ultraviolet (UV) light through masks (opaque support with transparent patterns). During exposure, the UV light chemical changes the illuminated SU-8 zones properties making the unexposed photoresist soluble to the developer. The photoresist patterns act as a master mould and can be impressed in PDMS by soft-lithography. A mixture of liquid pre-polymer and curing agent (PDMS) is cast against the master mould and peeled off after temperature curing creating a reversed replica of the master imprint. After punching the inlets and outlets zones, the PDMS is plasma-bonded on a substrate like glass slide and baked to help the covalent bonding of induced radicals between the PDMS and the glass slide after the sealing process [42]. All photolithography and soft-lithography processes are shown in Figure 2.2.

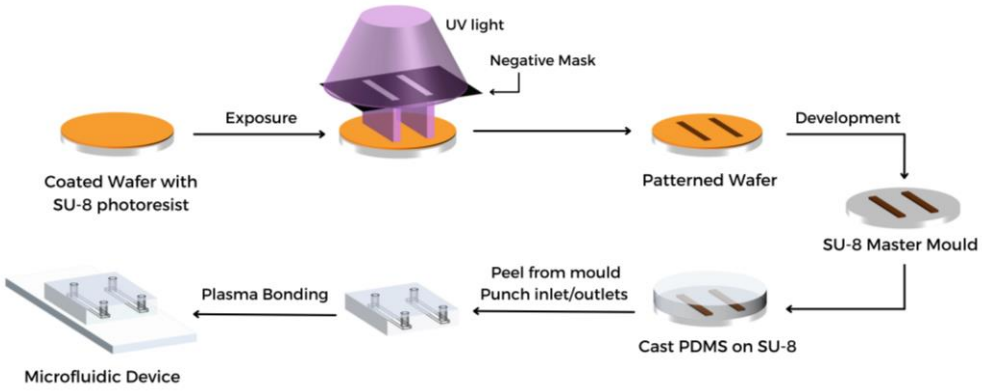

Figure 2.2 – Schematic representation of photolithography and soft-lithography and sealing procedures for the fabrication of PDMS microfluidic devices (adapted from [42]).

3. Materials and Methods

3.1 Chips Design

The chips layouts were optimized from previous work [43] and designed with the software Autodesk® Auto-CAD 2021. The channel design of the chips was not changed, since the fluidic behaviour was already known and it guarantees cells growth. Thus, only minor changes were made to improve its operation. In both layouts the outlets and inlets of the chips were increased to facilitate the perfusion with the puncher at microfabrication and in one of the layouts, the media channels' length was reduced after the tissue chambers to minimize clogging areas facilitating chip reuse.

3.2 Microfluidic Device Fabrication

All processes regarding the fabrication of the SU-8 mould, the PDMS microfluidic device, and the sealing (Figure I.1, Annexe 1) were executed within a class 1000 (ISO class 6, according to the US Federal Standard 209E and ISO 14644-1 standards [44]) micro and nanofabrication cleanroom yellow zone. All materials used in microfabrication were previously washed in ultrasound baths (Bandelin Sonorex) with acetone (LabChem) and isopropyl alcohol (IPA, Carl Roth GmbH) separately, dried by compressed nitrogen and baked at 180 ℃ on a hot plate (Clarkson HS40A-2, Torrey Pines Scientific).

3.2.1 Fabrication of the Master SU-8 Mould on Silicon Wafer by Lithography

The pattern of the chip's design was inscribed on a molybdenum hard mask by using a high-resolution laser printing (μpg 101 Tabletop Micro Pattern Generator, Heidelberg Instruments).

An epoxy-based negative photoresist SU-8 2050 (KAYAKLI Advanced Materials) was poured on the centre of a 4'' (10.16 cm) silicon wafer, previously washed, that was held in the centre of the spin-coater machine (KarlSuss Technique) by double face tape. Taking into account the thickness of the chip channels required (100 μm) and the room temperature (21.2 ℃), the protocol was a 2-step process: a pre-spun of 500 rpm for 7 s with an acceleration of 100 rpm/s, followed by a spun of 1620 rpm for 30 s with an acceleration of 300 rpm/s, where the spun speed was determined by the tables included in the SU-8 reference datasheet [45]. To evaporate the solvent of the SU-8 the wafer was subjected to a soft-baking process with two different temperatures: 65 ℃ for 5 min, and 95 ℃ for 16 min and removed to cool down before UV light exposure.

Using the hard mask previously fabricated, the sample was irradiated in a mask aligner (MA6, Süss MicroTec) with a 230 mJ/cm^2 dose of UV light (400 nm) for 39.3 s. The exposure time was calculated by dividing the exposure dose and the power density (5.85 mW/cm^2) that was previously detected with a UV-optometer (Süss MicroTec). To activate the cross-linker, the wafer was subjected to a 2-step post-exposure baking process with two different temperatures: 65 ℃ for 5 min and 95 ℃ for 10 min. At the end of this process, the pattern of the chip became visible. To dissolve the SU-8 in the unexposed regions of the wafer, it was developed in a constant agitation (50 rpm) bath of propylene glycol methyl ether acetate (PGMEA, Sigma Aldrich) on a universal shaker (Edmund Bühler GmbH) for 9 min. Afterwards, the wafer was rinsed with clean developer, IPA, washed with water, and finally dried with compressed nitrogen until no more photoresist is shown in the wafer. The wafer was analysed by optical microscopy (Axioscope 5, Zeiss) to verify if needed supplementary development. To remove possible cracks on the wafer, it was submitted to a post-bake process, where the wafer was baked at 150 ℃ for 30 min.

3.2.2 Fabrication of the PDMS Microfluidic Devices by Soft-Lithography

The PDMS master was prepared by mixing the base polymer (SYLGARD 184 Silicone Elastomer Base, Dow Corning) with the curing agent (SYLGARD 184 Part B, Dow Corning) in a 10:1 ratio and then de-gassed in a vacuum desiccator (Kartell). After removing the excess air bubbles, the mixture was poured over a silanized SU-8 patterned microfluidic casting mould (Chapter 3.2.1.) and placed again in the vacuum desiccator until no air bubbles could be seen on the surface. The mould with PDMS was placed into a levelled oven (Salvis Lab) at 80 ℃ to cure for 1 h. After cooling down to room temperature, the solidified PDMS was gently removed using an appropriate blade (Dexter) and slowly peeled off from the master mould by hand motion. Afterwards, the inlets and outlets zones of the PDMS microfluidic device were punched by a 1.25 mm diameter puncher.

3.2.3 Sealing Process

The PDMS microfluidic device was then oxygen plasma bonded to a previously washed glass slide (Menzel, Thermo Scientific) on the reactive ion etching with an inductively coupled plasma device (Phantom 3 RIE-ICP, Trion Technology) with a pressure of 1000 mT and radiofrequency of 25 W, where a purplish-blue colour plasma is generated for 70 s (Figure I.2, Annexe 1). The PDMS microfluidic device was manually put onto the glass slide, making some pressure on top, taking special attention to corners and baked on a hot plate at 110 ℃ for a minimum of 30 min with some weight on top of them.

3.3 Cell Culture

All processes regarding the cell culture (Figure II.1, Annexe 2) were executed in a vertical laminar airflow cabinet (Bio 48, Faster) and/or in a biological safety cabinets class 2 (ScanLaf Mars, Labogene) in a cell culture room. All materials were exposed to UV-C light (200 to 280 nm) for disinfection for 15 min after being sprayed with 70 % of ethanol (Valente e Ribeiro Lda.).

3.3.1 Fibroblasts Cells

For the growth of fibroblasts cells, Human Dermal Fibroblasts, neonatal (HDFn; Cellntec) (frozen in liquid nitrogen at 1 x 10^5 cell/mL, 1.5 mL per vial) and Mouse Embryonic Fibroblasts (MEFs; cells isolated in Chronic Diseases Research Center / NOVA Medical School (CEDOC/NMS)) were cultured separately in 89 % (v/v) of Dulbecco's Modified Eagle's Medium (DMEM; Gibco), supplemented with 10 % (v/v) of Fetal Bovine Serum (FBS; Gibco) to provide growth factors and a dose of Penicillin-Streptomycin (PS; Gibco) to prevent contamination in 1 % of the total volume.

Inside a 175 cm^2 surface area T-flask (T175), cells were added to 20 mL of media and placed into an incubator (Thermo Scientific Forma Infrared CO_2 Incubator) at 37 ℃ with a humidified atmosphere containing 5 % of CO_2 until the vial could be confluent under optical microscope visualization (about 90 % of the total seeding surface covered). Afterwards, the trypsinisation process started by removing the culture media and washing the surface of the T175 with 10 mL of Phosphate-Buffered Saline (PBS, Gibco) to remove the remaining DMEM. To detach the cells from the seeding surface, 3 mL of trypsin-EDTA solution (Gibco) was added to the flask and was placed into an incubator at 37 ℃, 5 % of CO_2 for 5 min. To block trypsin's effects, 7 mL of the media described initially were added. The cells were transferred to a 50 mL falcon (Deltalab) and centrifuged (Biofuge 28 RS, Heraeus) at 1200 rpm for 5 min at room temperature. After removing the supernatant and resuspending the pellet in 300 µm of media, the cells were in a suspended state. To estimate the number of cells present in the solution, 5 µL of the cell suspension was added to an eppendorf vial (1.5 mL), along

with 95 µL of Trypan Blue Solution (Sigma-Aldrich). 10 µL of that solution was pipetted to each counting chamber of a hemocytometer (Improved Neubauer 1/10 mm, Marienfeld Superior) that was utilized to count the viable cells placed on each of the four quadrants of its surface by optical microscopy (Eclipse TE 2000-S, Nikon). So that there was no overlapping of cells in the count, only the cells that were inside the square and on the top and left edges were counted (Figure II.2, Annexe 2). The estimated number of cells per mL was calculated by the following formulas:

$$C_i(cells/mL) = \frac{counted\ cells}{number\ of\ quadrants\ counted} \times Dillution\ Factor \times 10^4 \qquad \text{Equation 3.1}$$

$$Dillution\ Factor = \frac{V_{trypan\ blue} + V_{cells}}{V_{cells}} \qquad \text{Equation 3.2}$$

Knowing the final concentration (C_f), the volume required for seeding in the chip (V_f) and the initial concentration previously calculated (C_i), the volume of cells for culturing (V_i) was achieved by using the following formula:

$$C_i \times V_i = C_f \times V_f \Leftrightarrow V_i = \frac{C_f \times V_f}{C_i} \qquad \text{Equation 3.3}$$

3.3.2 Endothelial Cells

For the growth of HUVECs (cells isolated in CEDOC/NMS) de-frosted cells were cultured in Endothelial Cell Growth Medium-2 (EGM-2, Lonza, Endothelial Basal Medium-2 supplemented with EGM-2 Single-Quots supplements to provide growth factors). After 100 % confluency, a dose of PS is added to 1 % of the total volume of the EGM-2 to prevent contamination. Trypsinization and counting processes were similar to methods described in Chapter 3.3.1.

3.4 Seeding the Device

To prepare the hydrogel solution, fibrinogen from bovine plasma (Sigma-Aldrich) was dissolved in PBS reaching a final concentration of 10 mg/mL. The solution was dissolved in a 37 ℃ water bath (Waterbath B-480, Büchi) for 15 min and was then filtered with a 0.22 µm syringe filter (Acrodisc, Pall Corporation).

The estimated volume of cells for culturing (V_i) calculated with Equation 3.3 was transferred to an eppendorf vial (1.5 mL) and centrifuged (Biofuge 13, Heraeus Spatech) at 3000 rpm for 5 min at room temperature. After removing the supernatant, the cells were suspended in 13 µL of fibrinogen solution and mixed with 0.78 µL of thrombin from bovine plasma (50 U/mL, Sigma-Aldrich). To delay the fibrin reaction, the fibrinogen-thrombin-cells solution was prepared and maintained in ice [41].

The PDMS chip is transparent and the channels can be seen from outside. The chip was previously washed with IPA and PBS, then placed on top of a black surface to better follow the filling of the three chambers (Figure III.1, Annexe 3). 12 µL of the fibrin-cells solution was pipetted into the chip by applying a positive pressure in the cell inlet and put in the incubator (US Autoflow CO_2 Water-Jacketed Incubator, NUAIRE) for at least 45 min (Figure III.2, Annexe 3). To ensure that the fibrinogen-thrombin-cells solution fully polymerizes in the chip, the polymerization is verified by each chip assay. In a petri dish, 13 µL of fibrinogen solution were mixed with 0.78 µL of thrombin and allowed to fully polymerize. The solution was then optically analysed (Dino-Lite Edge) and if the fibrin became whitish, the polymerization was considered a success.

After the complete polymerization, the cells' inlet and outlets of the chip were covered up with transparent sealing film.

3.4.1 Automatic Oscillatory Feeding System

To guarantee a constant presence of culture media on the chip on a constant flow an automatic oscillatory feeding system was optimized. A 3D model of the system was designed in software Autodesk® AutoCAD 2021, converted to a 3D print using open source software Ultimaker Cura and printed layer by layer with polylactic acid (PLA) on a 3D printer (Ultimaker^{2+}). The system consisted of a platform where two containers delivered the media to the chip and maintained a height level difference between them. To become an automatic system an Arduino board (UNO R3, Geekcreit) controlled the movement using a servo motor (Micro Servo SG90, Tower Pro) and the system parameters were defined on an I2C communication protocol organic light-emitting diode (OLED) display menu by an EN-11 rotary encoder with centre-push before each assay (Figure IV.1, Annexe 4). All electronic components were inside of a plastic box for protection against the incubator's humidity.

2 mL of culture media was added to each 5 mL pistonless syringe (Braun Omniflix) attached to a 23G needle (Terumo® Agani) and tubing (Darwin Microfluidics), previously washed with IPA and PBS and taking special attention to removing air bubbles formed in the syringe by tapping carefully. The chip with the fibrinogen-thrombin-cells solution was positioned on the platform of the system and the media-filled tubing was inserted into the media inlet and outlet. Using one piston lightly pressed against the top of the syringe linked to the media inlet, the media flowed from the inlet to the outlet, removing the interior's chip air. To prevent media contamination, the tops of the syringes were covered with sterilized aluminium foil. After defining the parameters of the automatic feeding system (min: 80 º; max: 110 º; time: 24 h), the system was placed on an incubator and the media was substituted after 24 h and then every two days.

3.5 Characterization

3.5.1 Immunofluorescence Test

Two different immunofluorescence assays were performed however every immunofluorescence staining protocol consists of four major steps: fixation, permeabilization, staining and imaging.

In the first immunofluorescence assay to prevent disintegration and dispersion of the cellular content, 20 µL of 10 % Neutral Buffered Formalin (Bio-Optica) solution was injected into the media inlet and subsequently washed thrice with PBS. To stain intracellular proteins, the cell needs to be permeabilized, so 20 µL of 1 % Triton X-100 (USB - United States Biochemical Corporation) in PBS previously done (500 µL of Triton X-100 mixed with 49.5 mL of PBS) was injected into the chip and washed thrice with PBS after 15 min. The fluorescent stain added was 1 µg/mL of 4',6-diamidino-2-phenylindole (DAPI, Invitrogen) in PBS (1 µL of DAPI with 1 mL of PBS) and the chip stayed in the dark for 30 min before being optical analysed.

The last assay was an indirect immunofluorescence antibodies test and the initial processes were similar to the methods described above, apart from reagents. For fixation, it was injected 20 µL of 4 % Paraformaldehyde (PFA, Sigma-Aldrich) mixed with 0.5 % Triton X-100 and for permeabilization 20 µL of 0.1 % Triton X-100 in PBS. To block non-specific antigens 20 µL of Blocking Solution (BS; comprises 400 mL of PBS, 3 g of glycine (Sigma-Aldrich), 800 mg of bovine serum albumin (NZYTech) and 80 mg of sodium azide (Sigma-Aldrich)) was injected into the chip for one hour. The primary antibody added was 1:40 % (v/v) of Purified Rat Anti-Mouse CD144 (BD Pharmingen) in BS and after two hours' incubation to avoid background fluorescence it was washed with BS thrice with 15 min waits in between. A secondary antibody conjugated to a fluorophore, 1:50 % (v/v) of Donkey anti-Rat IgG (H+L) Alexa Fluor 488 (Invitrogen) in BS, was injected in the media inlet, let incubate and washed three times with BS. The chip was left in the dark before being analysed by a fluorescence microscope.

4. Results and Discussion

4.1 Microfluidic Devices

4.1.1 Chip Design

Two different layouts of the microfluidic device were design optimized and used to investigate the development of vessels inside “tissue chambers”. Both designs consisted of two fluidic channels separated by three diamond microtissue chambers (2 x 1 x 0.1 mm) connected in series (Figure 4.1 D). Each chamber is connected to the media channels through two communication hourglass-shaped pores (30 µm wide) on each side. The pores were designed to mimic a capillary burst valve to prevent hydrogel leakage into the media channels by forming a meniscus. However, if the driving force exceeds the resisting capillary force the meniscus can burst [28].

In one adaptation (Model I - Figure 4.1 left), the media inlet and outlet are connected by a direct fluidic channel. The microchannel line from one side of the last tissue chamber connects to the other side of the first chamber, and then consecutively to the remaining microtissue chambers in numerical order.

In the alternative design (Model II - Figure 4.1 right), the media is forced to flow through the tissue chambers since there is no straight connection between the media inlet and outlet.

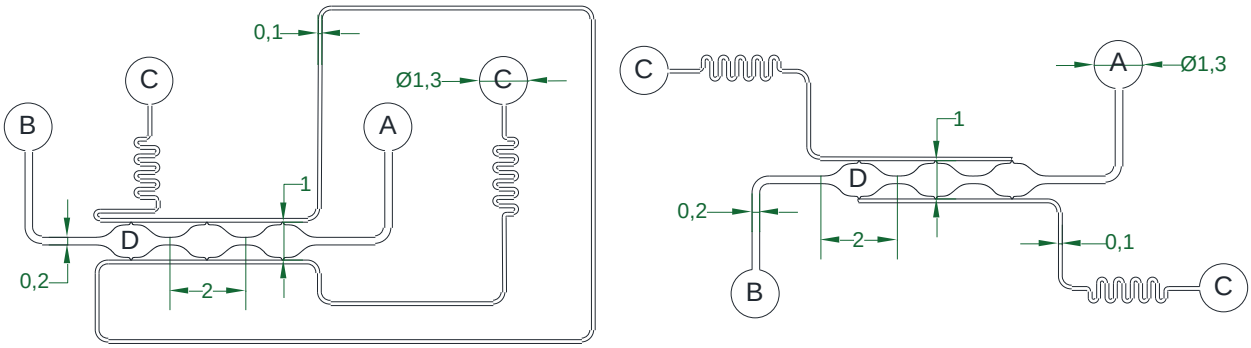

Figure 4.1 – Schematic of the microfluidic device design of (left) model I and (right) model II with dimensions in mm. A – Cells inlet; B – Cells outlet; C – Media inlet/outlet; D – Tissue Chamber.

4.1.2 Microfabrication

4.1.2.1 Hard-Mask Fabrication

The SU-8 mould was produced successfully incorporating four chips, two from each design, in a silicon wafer. Aimed thicknesses of 100 µm required the use of SU-8 2050 which has great viscosity (12900 cSt). In the spin-coating process, the photoresist should be poured into the wafer from proximity to prevent air bubbles from forming. The SU-8 processing is very sensitive to the variation of certain parameters. It was noticed that the variation of the ambient temperature has a great influence on the viscosity and, consequently, on the scattering of the photoresist. To obtain structures with thicknesses of approximately 100 µm, it was observed that an increase of 1 ºC in room temperature implied a decrease of approximately 130 rpm in the spin coating.

4.1.2.2 PDMS Chip Fabrication

To better facilitate the removal of the PDMS chip, the SU-8 patterned mould surface was first silanized with Trichloro(1H,1H,2H,2H-perfluorooctyl)silane (PFOCTS, Sigma-Aldrich) for 15 min on a vacuum desiccator. PFOCTS is a biocompatible polymer with superhydrophobic and antifouling properties preventing the attachment of the PDMS to the silicon.

4.1.2.3 Sealing

During the sealing process with oxygen plasma between PDMS and the glass slide, it was noted that some devices presented poorly sealed parts creating air bubbles between the PDMS and the glass. When the bubbles were not in connection with microfluidic channels, there was no problem since it wouldn't interfere with the experimental assay. However, it is possible to be seen in, as Figure 4.2 A, some chips showed unsealed zones next to the tissue chambers and media channels. To overcome this problem, it was necessary to press the centre of the chip outwards to release the air when placing it on top of the glass slide after bonding with oxygen plasma for a full chip adhesion to the glass slide (Figure 4.2 B).

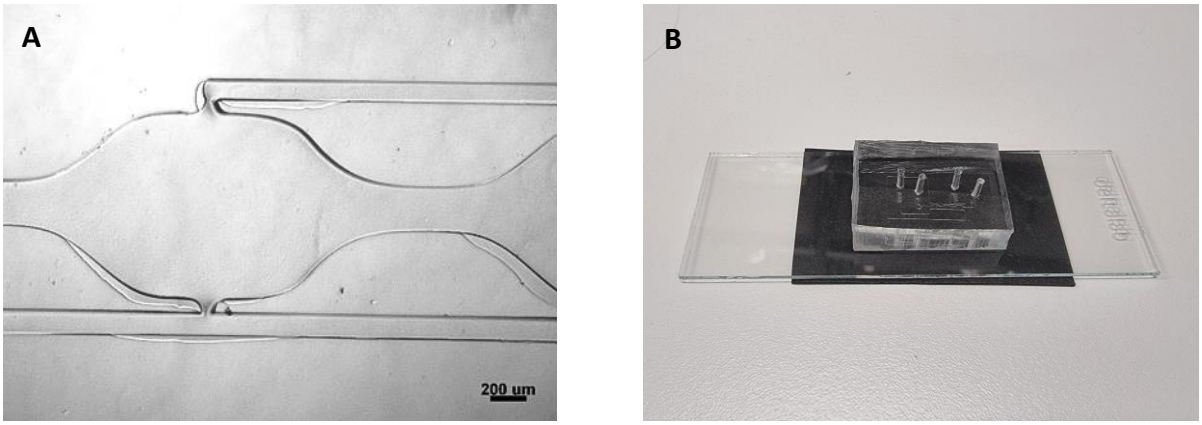

Figure 4.2 – (A) Zoom-in of the chip where it is noticed air bubbles caused by sealing problems; (B) Complete chip with a successful sealing process.

4.1.2.4 Chip Cleaning

Before each culture assay, it was necessary to clean the interior of the chip to minimize contaminations. The chips were cleaned with IPA and then repeatedly washed with PBS by applying a positive/negative pressure in the inlet and outlet, respectively with two micropipettes. For better removal of PBS traces, positive pressure in the inlets and/or outlets was applied using an empty syringe.

4.1.3 Chip Characterization

4.1.3.1 Hard Mask

The hard mask dimensions were characterized through an optical microscope. Figure 4.3 shows that the dimensions of the hard mask have suffered an increase when compared to design dimensions. There was an increase of 19.5 µm on average in media and cells channels, micron-sized zones, and in tissue chambers, millimetre-sized zones, an increase of approximately 0.15 mm on average. This increase in the dimensions of the mask will cause the fabrication of chips with dimensions slightly larger than the pre-sizing expected.

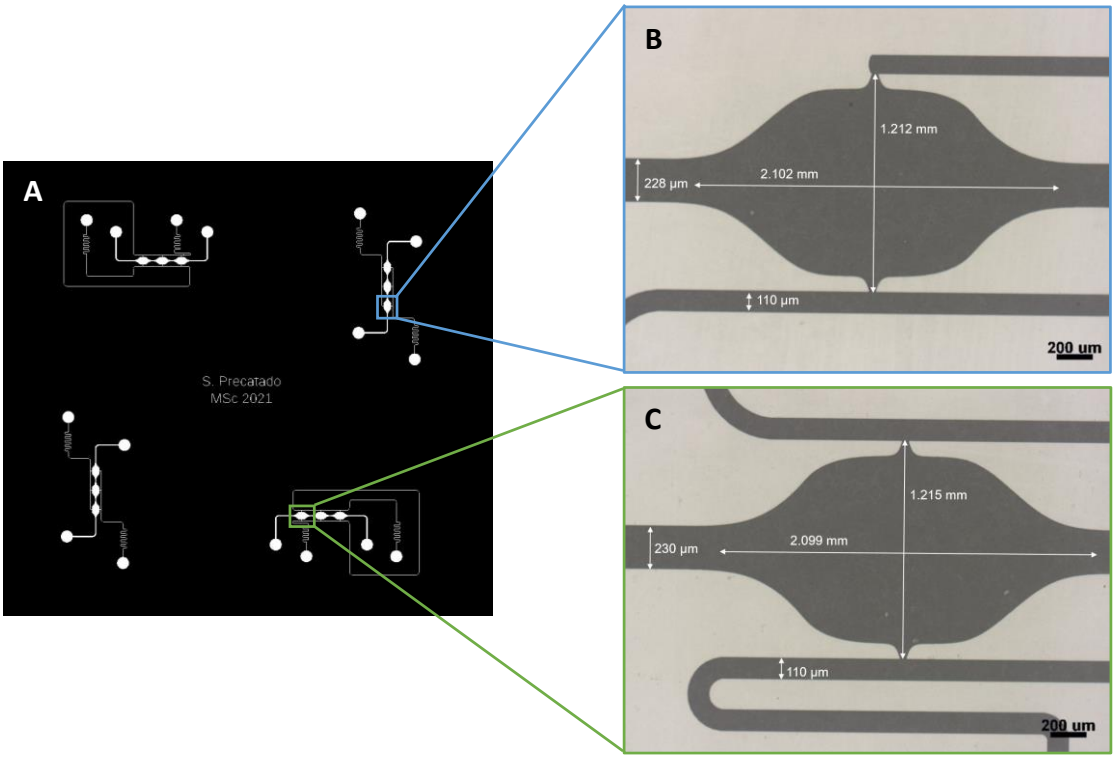

Figure 4.3 – Hard Mask dimensions. A) Hard Mask with four chips; B) Chip II Layout; C) Chip I Layout.

4.1.3.2 PDMS Device

The channel height was characterized through device cross-section analyse. To prevent spending more resources, the characterization was done on a damaged chip. The PDMS chip was cut perpendicularly to the channels and measured under the optical microscope (Figure 4.4 A). The measurements showed an increase of approximately 7 µm compared to the expected channel's height. This could be justified by an increase in the SU-8 thickness in the wafer due to a slight decrease in room temperature during the time of the spin-coating process. Additionally, it was possible to note that the sidewall is perpendicular to the bottom of the channel.

Measurements of the pore and chamber of the chips were performed as well (Figure 4.4 B). The pore width suffered an increase of 5 µm and the chamber dimensions increased by approximately 0.12 mm on average. Although the dimensions were larger than the pre-sizing, this increase was slightly smaller than expected after the hard mask characterization.

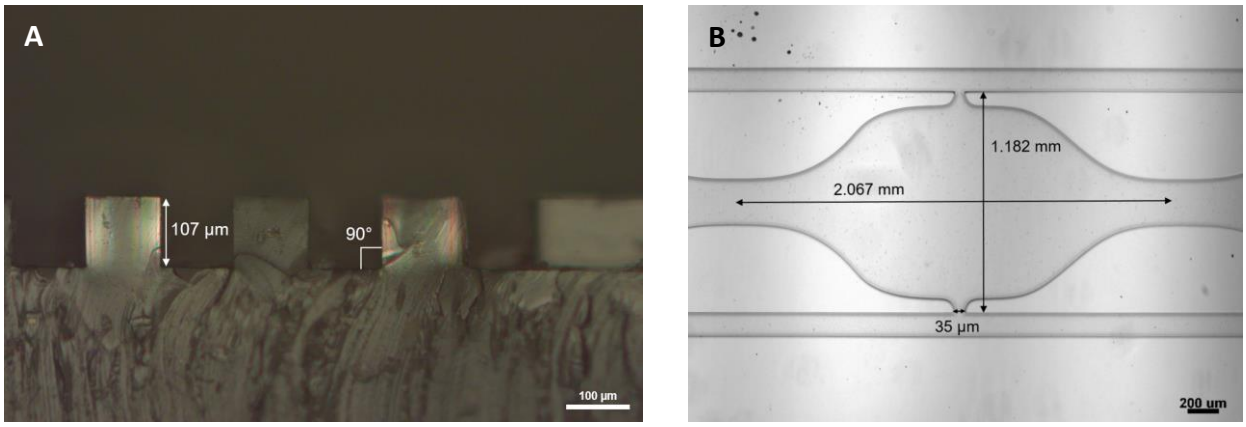

Figure 4.4 – Chip measurements using optical microscopy. A) Determination of channel height by cross-section analyse; B) Measurement of pore width and chamber width and length.

4.2 Automatic Oscillatory Feeding System

The culture media was delivered to the chip means a pressure gradient, promoted by an automatic oscillatory feeding system that allows uniform cell growth.

The feeding system setup (Figure 4.5) consisted of two parallel beams connected to two syringes supports on each side where four reservoirs with the media could be fixed. Initially, the system was designed to feed one chip. To increase the experimental capacity, an improvement was made by doubling the number of media containers that can be held in each support, allowing two experimental assays simultaneously and reducing the waiting time between assays

The bottom beam of the system was connected by an acrylic cylinder to a wheel that was attached to a servo motor (Figure 4.5 A). The servo is an electromechanical actuator designed for high precision positioning motion control, fast reversing and high performance. An Arduino microcontroller board controlled the servo motor to achieve a culture media level difference and therefore the pressure gradient necessary for uniform cell growth.

Before each assay, the operation parameters of the system were defined on an OLED display menu by using a rotary encoder with a centre push (Figure 4.5 B). Pressing the encoder allowed scrolling through the different parameters and rotating it to select different options. When setting a number, turning the encoder clockwise the number will increase, and turning counter-clockwise the number will decrease. This menu presented an accessible user interface where it was possible to define the setting of three important system parameters: (i) the servomotor rotation angles (min and max) and therefore the level difference between media reservoirs; (ii) the time, in hours, between the change of flow direction (time) and (iii) the initial direction of the media flow (side: left or right). The last menu option allowed starting the system (start). The Arduino code used to control the automatic culture system is presented in Figure IV.2, Annexe 4.

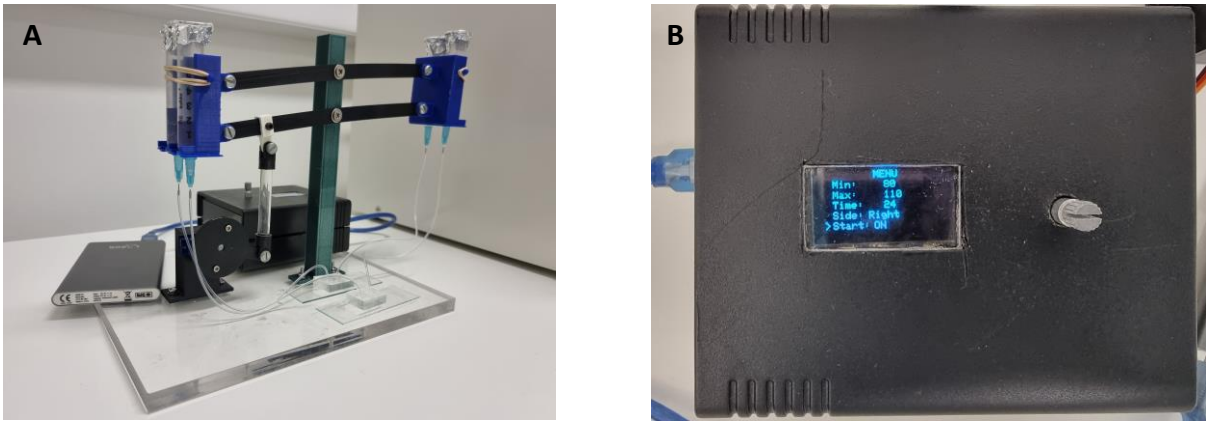

Figure 4.5 – (A) Complete Automatic Oscillatory Feeding System with supporters for two syringes each; (B) Box close-up with the OLED menu and the rotary encoder with centre push.

4.3 Experimental Assays

4.3.1 Cell Culture

Since cells have a central role in the course of the proposed study, cell growth was monitored every 2 days until achieving an approximate value of 100 % of confluency. Figure 4.6 shows images of HDFn plates on day 0 (A) and until achieving confluency on day 11 (B). Images of MEFs and HUVECs confluency can be found in Figure II.3, Annexe 2.

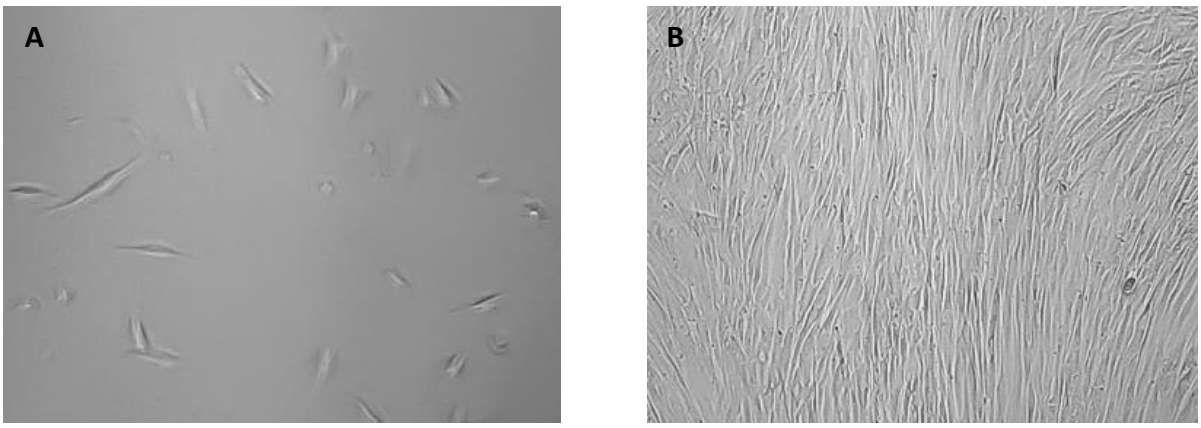

Figure 4.6 – HDFn cell confluency from (A) plating day until (B) 100 % of confluency.

Before each assay, it was required cell trypsinization since this routine allows adherent cells to become in suspension within the culture media. This process was found possible after three or four media exchanges. It was noted that for HUVECs, it was necessary to add a 5 min incubation after PBS wash before the introduction of trypsin since these cells have more difficulty to de-attach from the substrate.

4.3.2 Fibroblast Assays

To optimize the experimental protocols, several assays with HDFn were performed. These assays made possible to understand the introduction of the mixture of hydrogel and cells in the tissue chambers, the cell seeding and behaviour in the chip and the best method for the culture media passage.

4.3.2.1 Loading Device

After cell culture and expansion, seeding the device was the next step. 30 µL of the hydrogel-cell mixture was micropipetted in the inlet and outlet of the tissue chambers using positive/negative pressure, respectively. The pressure needed to be steady and even to avoid mixture leakage into adjacent media channels and the creation of air bubbles (Figure 4.7 A). If media channels were filled with hydrogel and cells or chambers had several air-hydrogel interfaces, media did not go through leading to cellular necrosis in the chambers. Therefore, when the filling process did not went as planned it was necessary to repeatedly wash the chip with PBS to remove the hydrogel-cells mixture and restart the process.

To prevent air bubbles formation that avoids the media passage, in the filling process with the hydrogel and cells mixture the cell lines needed to be completely full (Figure 4.7 B).

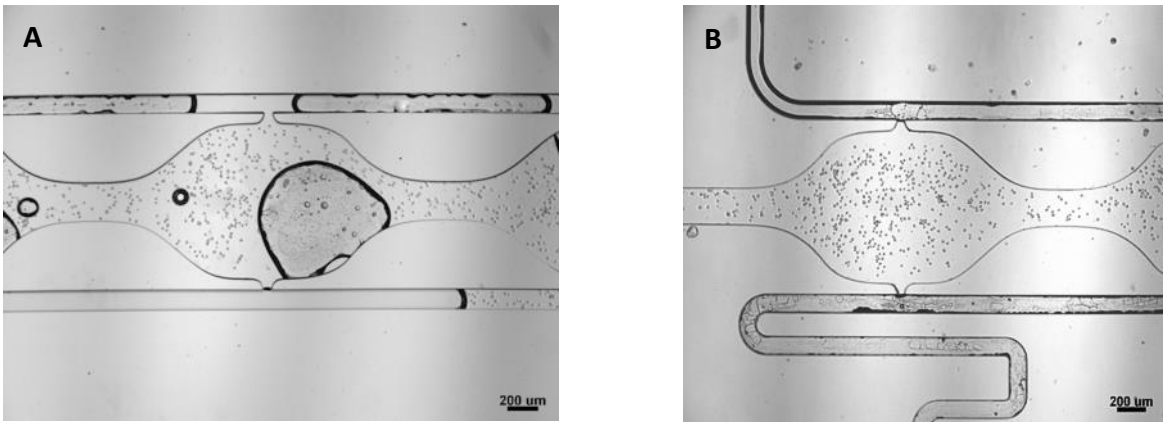

Figure 4.7 – (A) Leakage of hydrogel and cells mixture into the media channel and air bubble formation; (B) Proper loading of the device.

4.3.2.2 Hydrogel Polymerization

Cell attachment is a crucial step in microfluidic cell culture. Ensuring good attachment of the cells to the tissue chamber of the chip, avoid the cells being washed away when the culture media is flowing through. Therefore, it was important to determine the optimal time of hydrogel polymerization to catch the cells at the right moment.

To determine the polymerization time of the fibrin-thrombin-cells mixture, a polymerization test was performed before the chip assay. However, it was noticed that fibrin and thrombin underwent degradation after repeated thawing and freezing. Thus, several aliquots of 20 µL of thrombin and 400 µL of fibrin were made to minimize the effects of degradation and the polymerization test was performed simultaneously with each assay. Additionally, it was observed in case of contamination occurs, hydrogel does not fully polymerize and regresses in area and volume (Figure 4.8 A-D). When in chip assays, the regression of the hydrogel creates an interface that prevents the growth of cells leading to their death (Figure 4.8 E).

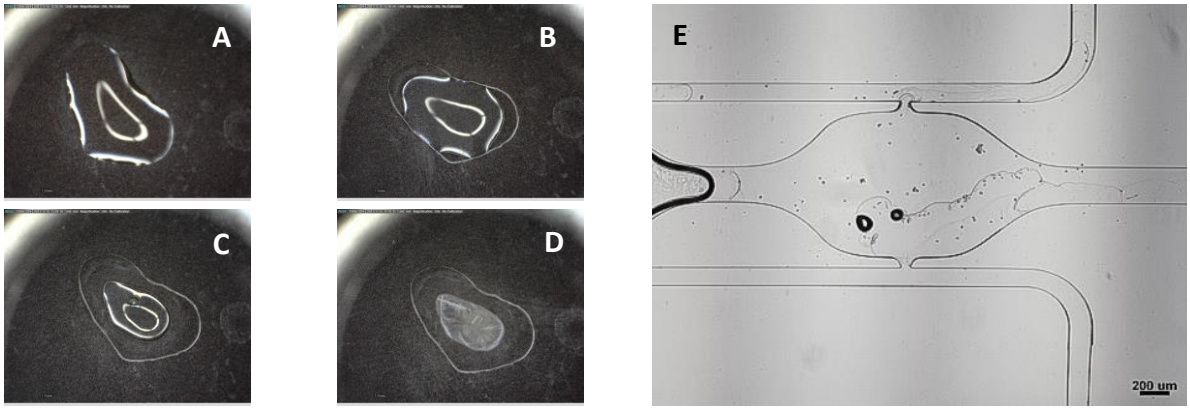

Figure 4.8 – Polymerization regression. (A) Initial time; (B) 30 min; (C) 60 min; (D) 90 min; (E) HDFn assay.

A good polymerization occurs when the mixture retained its volume and became whitish. Experiments demonstrated that it was necessary at least 45 min at 37 °C with a humidified atmosphere containing 5 % of CO_2 to fully polymerize resulting in a quarter-hour increase related to the time described in the literature [26].

The Figure 4.9 shows the difference observed in tissue chambers after introducing culture media at different times of polymerization incubation at 37 °C. In Figure 4.9 A, the polymerization time was 30 min, while in Figure 4.9 B, the chip was 45 min in the incubator. In the first case, almost no cells were observed in the tissue chambers as their entrapment in the polymer was not completed and had been washed away by the culture media flow; while in the latter, the fibrin-cells mixture was completely polymerized catching the cells in the tissue chambers.

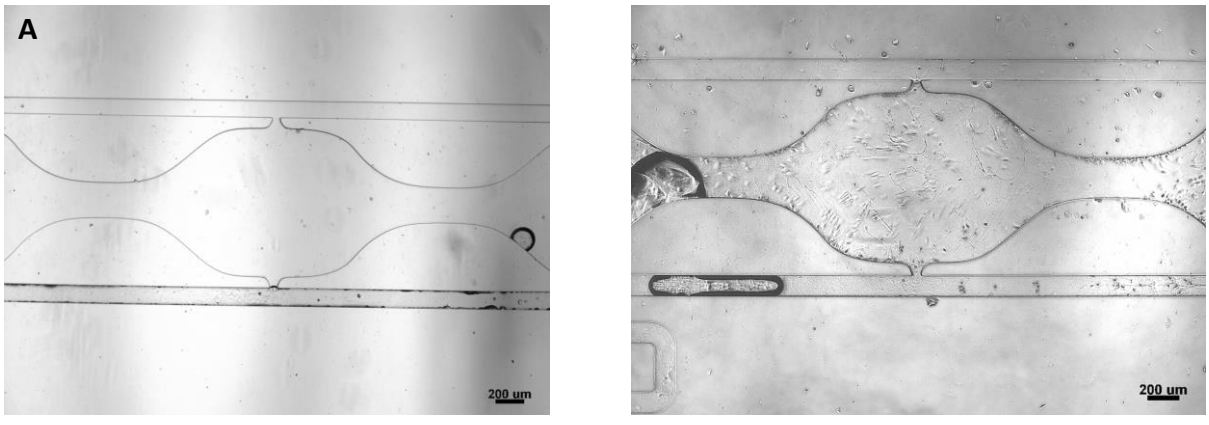

Figure 4.9 – Tissue chambers of different assays after introducing culture media after a cell-hydrogel mixture polymerization of (A) 30 min and (B) 45 min.

4.3.2.3 Culture Media

To promote the proliferation and viability of cells, a continuous flow of culture media needs to be established through the cells in the tissue chambers.

The media was introduced into fluidic lines by fluid-filled tubing connected to the reservoirs. To avoid interrupting the passage of the culture media through the microfluidic device, the media within the syringe and tubing needed to be free of air bubbles. On that account, before introducing the media into the chip, the filled reservoirs had to be tapped to release trapped air bubbles and then connected to the tubing to flow the media through.

Different strategies were tested to introduce culture media into the microfluidic device to prevent the formation of air bubbles inside de chip. The media-filled tubings were connected to the chip media inlet and outlet and the air inside the chip was removed after applying a steady even pressure to one of the syringes. It yielded positive results despite having a small setback that was necessary to pay attention to. It was necessary to remove the air bubble coming from the chip interior that was lodged in the needle and syringe by tapping carefully. Although this method was tested to eliminate the air inside the chip when the culture media was introduced, some assays showed air bubbles in the tissue chambers. When air bubbles were small in size and number, it was noticed that they vanished in the next hours after media passage. However, when contamination occurs after a few hours the air bubbles spread all over the chip preventing the passage of the medium and leading to cellular death.

The media flowed through the tissue chambers and was levelled every 24 h by the media delivery system. This media reservoir position change induces a pressure difference that created an average flow rate of 0.329 ± 0.079 µL/min in the chip. This flow rate allowed HDFn proliferation inside the tissue chambers.

4.3.2.4 Cell Concentration

To understand the behaviour of the cells inside the chip related to the cell population, different concentrations of HDFn were tested (Table 4.1).

Table 4.1 – Final cells concentration, the volume pipetted and the number of cells of different HDFn assays.

C_f (cell/mL)	V_f (µL)	Number of cells
7.500×10^6	30	22.500×10^4
3.750×10^6	30	11.250×10^4
5.625×10^6	30	3.875×10^4

Initially, a concentration of 7.500×10^6 cell/mL was seeded into the chips and after a few assays, it was possible to verify the high confluence of cells after seven days of feeding by the oscillating culture media. Figure 4.10 A shows the growth of HDFn in the tissue chamber and their proliferation into the media channels after 11 days.

The concentration of 3.750×10^6 cell/mL in different assays showed air/media interfaces that impeded the passage of the culture media which eventually lead to cellular necrosis. Figure 4.10 B show this observation by the contrast of the area inside the chip occupied by air (grey), the media culture (pink) and their interfaces (black). Cells need a culture medium to grow and proliferate and since most of the chip area was filled with air, it occurred the death of all seeded cells. The air bubbles' creation and dispersion through the chip can be explained by some causes: (i) the seeding and the culture media passage protocols were not fully optimized at that moment and (ii) contamination in the chip was also detected, which could have developed gas production

inside the chip. Despite not having been visible the creation of a network of organized and grown cells with this concentration of cells, the experimental assays were important to optimize the protocols and procedures for assays with the chips.

Lastly, a concentration of cells of 5.625×10^6 cell/mL was seeded into the chip and after culturing for 12 days, with the oscillating culture media feeding with an average flow rate of (0.33 ± 0.07) µL/ min, it was observed an interconnected network of grown cells in the tissue chambers. From day 12 to 22, the grown cells proliferate into the media channels occupying all areas of the chip (Figure 4.10 C).

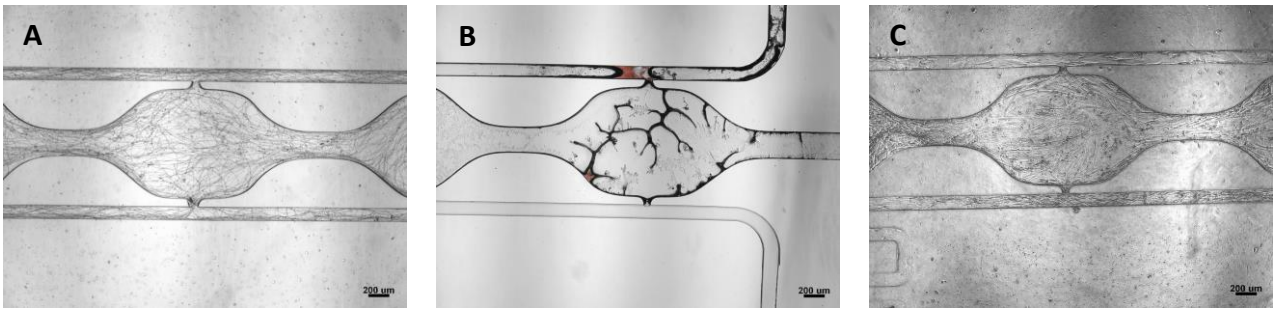

Figure 4.10 – HDFn assays with cell concentrations of (A) 7.500×10^6 cell/mL, (B) 3.750×10^6 cell/mL and (C) 5.625×10^6 cell/mL.

Since there was not possible to visualise the creation of an interconnected network of fibroblasts with 3.750×10^6 cell/mL of concentration due to external conditions to the assay, it would be inaccurate to state that this concentration of cells is not enough for cells growth and proliferation inside the chips. However, with the results of other concentrations assays, it could be stated that the time it takes to create cellular networks with a 24 h oscillating culture media feeding is intrinsically linked to the concentration of cells. The lower the concentration of fibroblasts seeded in the chip, the longer it takes for their growth.

4.3.2.5 Immunofluorescence Test

In the assay with a cell concentration of 3.750×10^6 cell/mL, the presence of air bubbles was not noticed; however, the presence of unknown composites was observed in the cell chambers. An immunofluorescence assay was carried out to identify living cells inside the microfluidic device. DAPI was the label chosen for the immunofluorescence assay, as it binds directly to the deoxyribonucleic acid (DNA) of the cellular nuclei of fixed cells resulting in bright blue fluorescent emission from the nucleus of living cells and no detectable fluorescence from their cytoplasmic fluid [46].

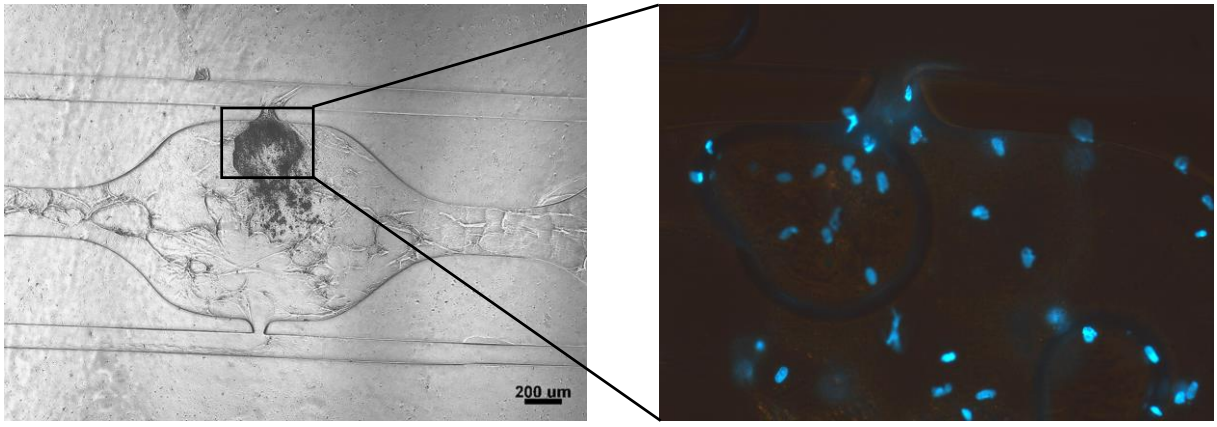

Figure 4.11 – Immunofluorescence assay with DAPI using a fluorescence microscope where the blue dots represent the cellular nuclei of fixed cells.

The Figure 4.11 shows that even though there was a high concentration of unknown composite in the tissue chambers, presumably contamination, numerous blue dots were observed under a fluorescence microscope making it possible to verify the cell culture and growth success. However, determining the presence of cells inside of a microfluidic device using DNA fluorescent stain has the drawback of being an endpoint assay since the cells need to be fixed stopping the cell growth and the assay.

4.3.2.6 Contamination Threat

Contamination is one of the main concerns when developing a cell culture on an *in vitro* assay since it adversely affects the quality of the results. It can cause adverse effects on the cells that lead to inaccurate experimental results and, obviously, loss of time, resources and effort spent setting up experiments. During the optimization of the protocols, is was observed different contaminations effects during the assays: the hydrogel polymerization regression and the gas production creating air bubbles. During one of the assays, contamination was also observed in the media syringe which spread to media channels and eventually to tissue chambers (Figure 4.12 A and B). Despite antibiotics being added to media culture to prevent biological contaminations, a microorganism was colonized and prospered in the rich environment of media culture.

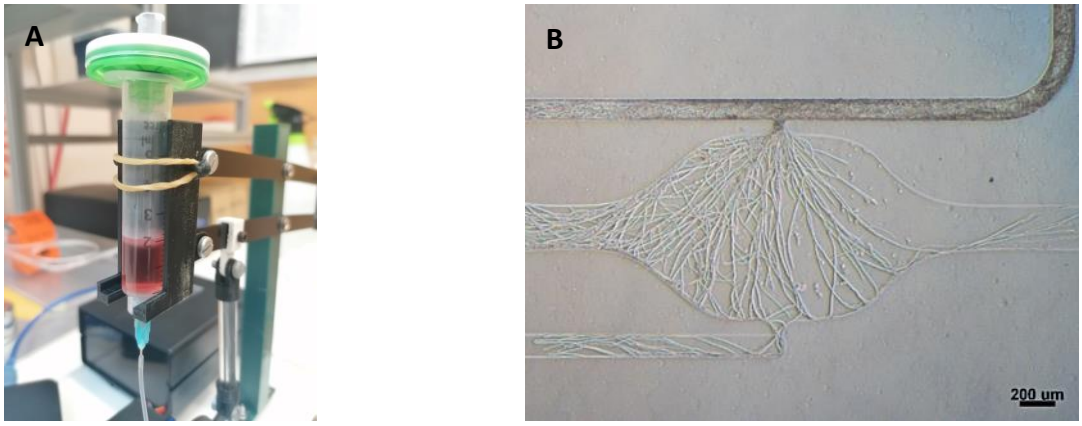

Figure 4.12 – (A) Contamination in the media syringe detected by direct visual observation; (B) Contamination spreading through the chip.

As Ryan J. says "contamination cannot be totally eliminated, but it can be managed to reduce both its frequency of occurrence and the seriousness of its consequences." [43, p. 2]. So to reduce the frequency of biological contamination it was important to understand the origin of the contaminants and how they were able to access cultures.

Incubators can be a major source of biological contamination since dirty water reservoirs at the incubator's bottom can induce the growth of spore-generating fungi that can be spread to the media by air circulation. Unsealed media reservoirs, in this case, syringes provide another approach for contaminants to access cultures since the media of the syringe can condensate creating a rich environment for microorganisms to grow and proliferate into the media and eventually the chip.

Therefore, after cleaning and decontaminating the incubator and replacing the use of unsealed syringe filters as syringe caps with sterilized aluminium foil to minimize the exposure of media to air, contamination was no longer a major threat during experimental assays.

4.3.3 Endothelial Assays

The goal of this work was to achieve an interconnected human capillary network, so after optimizing seeding and media passage protocols, several assays were performed with endothelial cells (HUVECs) and fibroblasts (MEFs) as support.

4.3.3.1 Loading Device

When micropipetting 30 µL of the hydrogel-cell mixture in the microfluidic device using positive/negative pressure (Figure 4.13 A), it was observed a lower number of cells inside the chambers as a result of the wastage of cells at the tips during the loading procedures. It was noted that micropipetting the real volume of the tissue chambers and cell channels, 12 µL, of the hydrogel-cell mixture into the cell's inlet by positive pressure allows the total cell entry in the chambers (Figure 4.13 B).

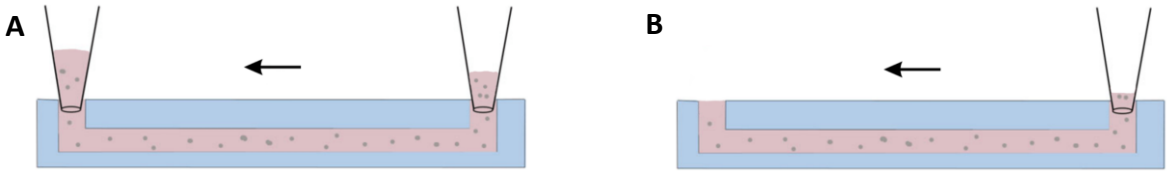

Figure 4.13 – Different loading techniques. (A) Positive/negative pressure in the inlet/outlet of cells, respectively; (B) Positive pressure in the inlet of cells (adapted from [41]).

4.3.3.2 Vessel Network Formation

Several cell concentrations in different proportions of HUVECs and MEFs, shown in Table 4.2, were tested towards finding the right proportion of cells to achieve a capillary network.

Table 4.2 – Final cells concentration, the volume pipetted and the number of cells on each endothelial assay.

C_f (cell/mL)		V_f (µL)	Number of cells	
MEFs	**HUVECs**		**MEFs**	**HUVECs**
5.00×10^6	2.50×10^6	30	15.00×10^4	7.50×10^4
5.00×10^6	2.50×10^6	12	6.00×10^4	3.00×10^4
7.50×10^6	3.75×10^6	12	9.00×10^4	4.50×10^4
5.00×10^6	1.00×10^7	12	6.00×10^4	12.00×10^4

Initially, experimental assays were performed by seeding more fibroblasts than endothelial cells. Based on previous studies [30], [41] two assays with a concentration of 5.00×10^6 cell/mL and 2.50×10^6 cell/mL of MEFs and HUVECs, respectively, were performed. The main difference observed in Figure 4.14 A and B is related to the number of cells that entered the chip. The second assay (Figure 4.14 B) exhibited a bigger number of cells inside the chip since there was no wastage of cells at the tips during the insertion of the hydrogel-cells mixture into the chambers. It was observed that this concentration of HUVECs supported by the co-cultured MEFs did not integrate into vessel networks after an average culture media flow of 0.121 µL/min. Previous studies have demonstrated the generation of an interconnected network of capillaries with a ratio of 2:1 of fibroblasts and endothelial cells suspended in fibrin-thrombin gel [30]. However, the kind of cells for culture used by Moya et al. [30] was different from those used in this work, which can be a reason for the non-formation of vessel networks.

Therefore, it was increased the number of cells in the microfluidic device to better understand the impact of this HUVECs:MEFs ratio. Increasing the cells' concentration to 7.50×10^6 cell/mL and 3.75×10^6 cell/mL of MEFs and HUVECs, respectively, and after 14 days of culture in the chip, did not evidence the creation of a network of capillaries (Figure 4.14 C).

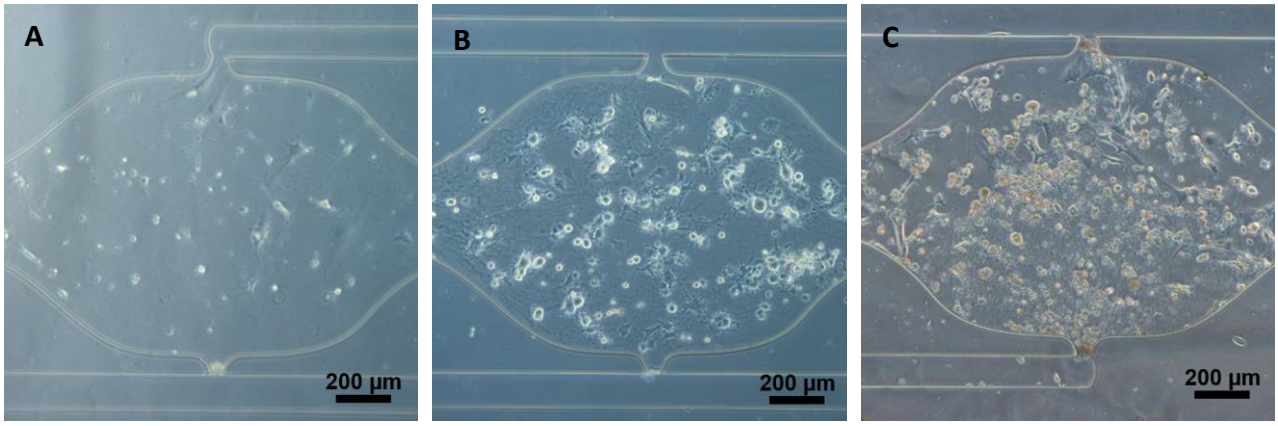

Figure 4.14 – Microscope images of assays at a ratio of 2:1 of MEFs and HUVECs. (A, B) Concentration of 5.00×10^6 cell/mL of MEFs and 2.50×10^6 cell/mL of HUVECs and with different volumes of the chambers and cell channels: (A) 30 µL and (B) 12 µL. (C) Concentration of 7.50×10^6 cell/mL and 3.75×10^6 cell/mL of MEFs and HUVECs, respectively with a volume of 12 µL after 14 days of culture.

Therefore, a second proportion between endothelial cells and fibroblasts concentrations was tested by keeping the 5.00×10^6 cell/mL of MEFs and increasing the HUVECs concentration to 1.00×10^7 cell/mL, with a ratio of 1:2 [26]. After 14 days of culture with an average media flow of 0.385 µL/min, it was possible to observe signs of the development of an interconnected vessel network within the microfluidic device. The HUVECs aggregated into tube-like structures in the first 24 h (Figure 4.15 A) and after 14 days the microvessel network in all chambers grew toward both pores (Figure 4.15 B) and interconnected the three diamond-shaped tissue chambers (Figure 4.15 C). The vessel networks formed were not fully continuous, but nevertheless, it suggests that this concentration has a vasculogenic potential.

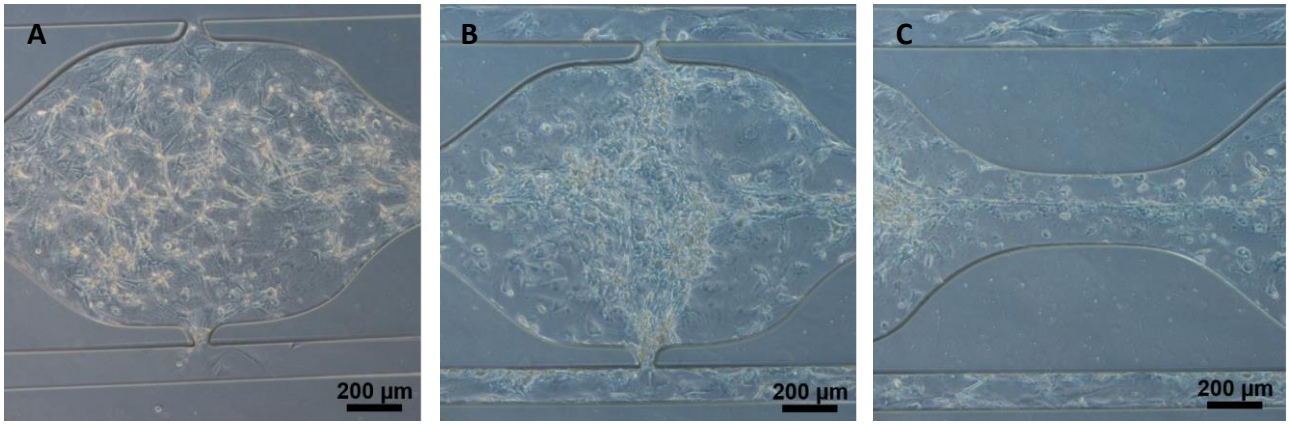

Figure 4.15 – Microscope images of the signs of vessel network formation with MEFs and HUVECs on a ratio of 1:2 after (A) 24 h and (B)(C) 14 days.

An immunofluorescence assay was carried out to identify the vessel network. The DAPI stain was used to detect the cellular nuclei of both cells (Figure 4.17 B). To specifically identify the endothelial cells an indirect immunofluorescence assay with CD144 antibody was performed (Figure 4.17 C). This method consists of the use of two antibodies to label a target antigen with a fluorescent dye (Alexa Flour 488). In this assay, the

primary antibody binds to the antigen and a fluorophore-conjugated secondary antibody recognizes and binds to the primary antibody (Figure 4.16) [48].

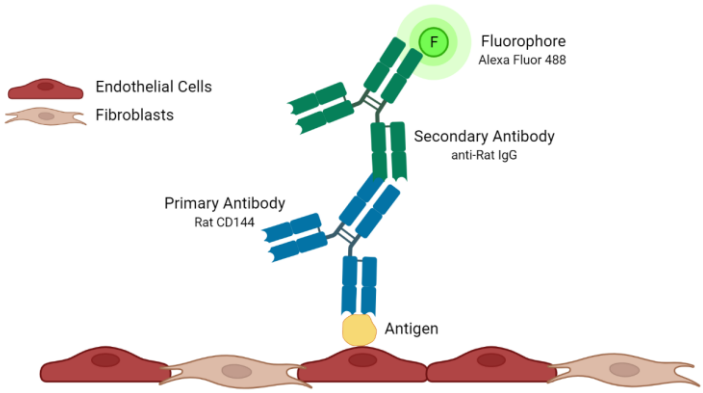

Figure 4.16 – Schematic of the principle for indirect immunofluorescence assay [Figure created with Biorender.com].

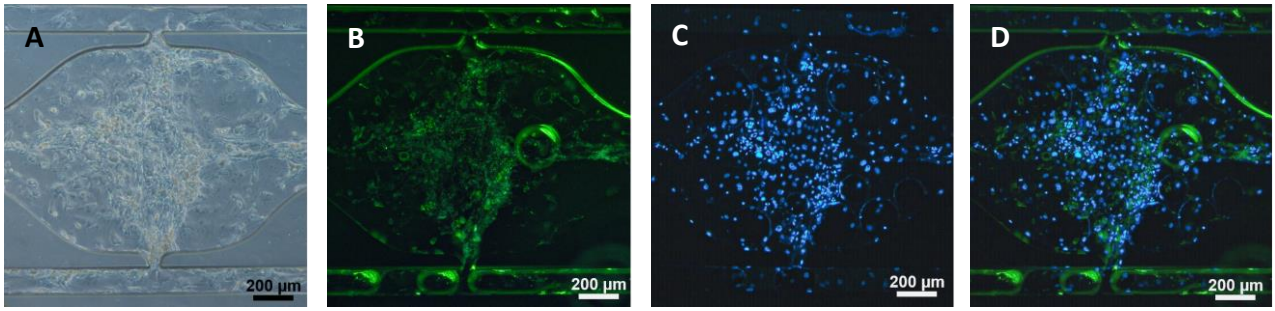

Figure 4.17 – Immunofluorescence analysis. (A) Bright-field image of the tissue chamber; (B) Endothelial cells were stained for CD144; (C) Cellular nuclei were stained by DAPI; (D) Overlay of both immunofluorescence images.

The image of the immunofluorescence assay Figure 4.17 shows that after 14 days of culture media feeding, the co-cultured HUVECs and MEFs in a ratio of 2:1 started to develop an interconnected vessel network despite not being a continuous and viable one. However, since previous studies [27], [30] had demonstrated the formation of viable networks of vessels with ECs and fibroblasts as support, it was necessary to understand that although the protocols have been previously optimized with fibroblasts, there is a need to further adapt and improve the protocols for assays with ECs.

In the image of Figure 4.17 D, it is possible to notice a major linear cell organization through the pores, which can be an indication of insufficient culture media flow. Since the medium enters the chambers through both pores, any constriction in the media flow limited the spread of media across the tissue chamber and the cells tend to agglomerate in the centre where the flow is greatest. Another evidence of insufficient culture media flow can be the propagation of cells through culture media channels. If the media flow is not sufficient to feed the cells into the chambers it can cause entropic growing of cells towards culture media channels that are loaded with media.

It was observed that the flow rate of culture media in all the assays with ECs was not uniform during the period of oscillating feeding not demonstrating a significant change between the two designs of the chip. As Figure 4.18 A shows the culture media flow rate peaked in the first few days of the experiments and then gradually began to decline. The average media flow rate of all ECs assays was 0.293 µL/min, which is very low compared to the literature (10 µL/min) [28]. Therefore, it is essential to determine strategies to improve and increase the culture media flow rate in future works such as (i) increasing the width of media channels in both

chip designs to increase the available area for flowing media; (ii) increasing the media flow pressure by increasing the level difference between reservoirs or iii) increasing the pressure by using a syringe pump delivery of culture media.

Another strategy to optimize the culture media flow could be shortening the time between the changes in the flow direction during the experimental assays. In Figure 4.18 B can be seen that the greatest media flow interval is comprised between the first 12 hours, thus shortening the flow oscillation period from 24 hours to about 12 hours will increase the amount of fresh culture media available to the cells. Figure 4.18 B shows the results of an assay tested with water on an empty chip (no polymer and cells in between). The graph in Figure 4.18 B does not meet expectations, since theoretically on a chip filled only with water, the flow would be maximum at the beginning of the assay and then gradually decrease. The increase in flow to its maximum value in the first 4 hours can be explained by the presence of small air bubbles in the channels and later in the tubing hampering the water passing through, which was also observed in the assays with cells.

It was also noted that after replacing the syringe supporters from 1 to 2 syringes each and after some time of use, the horizontal beams of the automatic feeding system began to slightly bend, reducing the difference in level between the reservoirs hence the pressure gradient that allows the media to flow through the chip. Thereby the horizontal beams of the oscillatory feeding system need to be reinforced to support the reservoirs with the culture media.

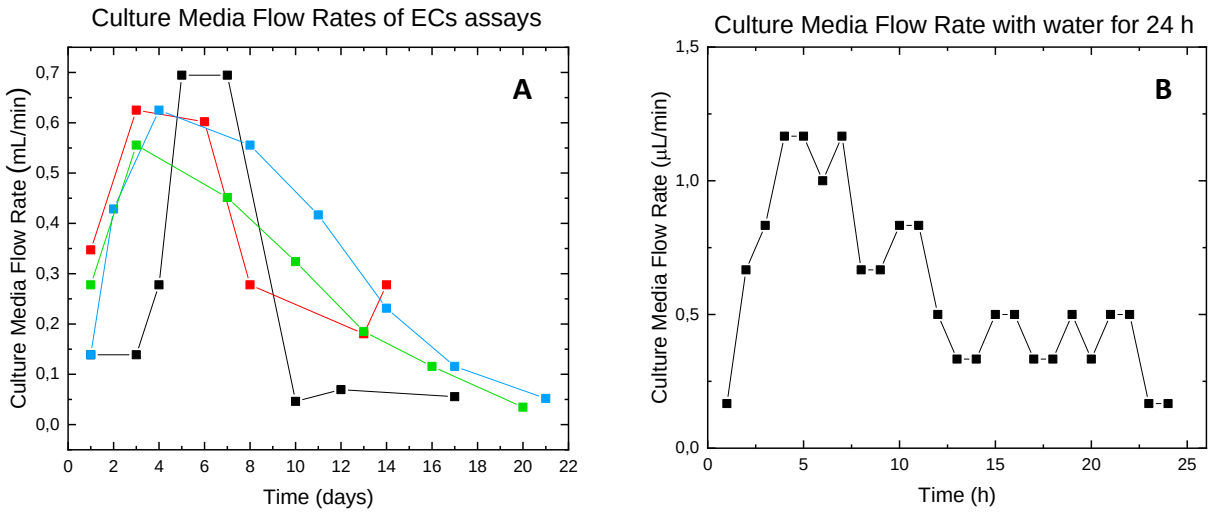

Figure 4.18 – (A) Culture media flow rates of different experimental assays with HUVECs and MEFs; (B) Culture media flow rate test on an empty chip with water for 24 h.

Taking into consideration the obtained results of the endothelial assays, a hydrogel contraction in the chambers can be observed in the four corners of the tissue chamber (Figure 4.17 A) and may also be the cause of cells' linear agglomeration. With the aim of minimizing fibrin degradation inside the chip, an enzyme inhibitor such as aprotinin can be added to the hydrogel mixture [26]. Despite Mühleder et al. [49] demonstrate that aprotinin in cell culture supernatant inhibits fibrin degradation, it can impair vascular network formation regarding the number of junctions, tubules and vessel diameter.

While the fibroblasts secrete growth factors including vascular endothelial growth factor (VEGF) that promote ECs proliferation, additional purified protein such as CCBE1 into the culture media may be necessary to promote better vascular development. CCBE1 is an extracellular matrix protein that has shown a robust vessel network formation *in vivo* [25] and *in vitro* [49].

5. Conclusions and Future Perspectives

This master thesis work was intended to optimize a microfluidic platform capable to develop a 3D human microvessel network of co-cultured ECs and fibroblasts.

A set of two different layout designs of microfluidic devices that allow cell growth were redesigned and fabricated through soft and photolithography. The results of the microfluidic chips characterization revealed that the microfabrication process is feasible resulting in great device reproducibility.

With the objective to ensure a constant flowing of culture media inside the microfluidic device that promotes uniform cell growth, an automatic oscillatory feeding system was optimized creating a pressure gradient by maintaining a difference in level between two culture media containers. An improvement was made by doubling the number of media containers that can be held in each supporter, allowing two experimental assays simultaneously and reducing the waiting time between assays. The system was built economically, the components constructed by 3D printing and operated by a servo motor connected to a microcontroller board and automatically changing the positions of the culture media containers every 24 hours. The culture media flow, direction and the time interval between positions can be defined before each assay by an accessible user menu on the platform. The setting time of the automatic oscillatory culture media delivery allows this platform to be used with other cell types without the need to change the Arduino code.

Initial assays were performed with different concentrations of fibroblasts to define the suitable experimental parameters. Therefore, the time of hydrogel polymerization, the cell seeding and culture media protocols were adjusted. It was possible to demonstrate that the growth of cellular networks is inversely related to the concentration of cells. The lower the concentration of fibroblasts seeded in the chip, the longer it takes for their growth.

After the optimization of the assays protocols, different concentrations of MEFs and HUVECs were combined with fibrin-thrombin hydrogel and seeded into the chips. A concentration of 5×10^6 cell/mL of MEFs and 1×10^7 cell/mL of HUVECs demonstrated a vasculogenic potential after 14 days of culturing with the oscillating feeding system, with an average culture media flow of 0.385 µL/min. The evaluation of the assay presented signs of cell growth mimicking an interconnected network of blood vessels, despite not being a complete viable one. The microvessel network in all chambers grew toward both pores and between the three diamond-shaped tissue chambers. The linear cell organization through the pores, confirmed by the immunofluorescence analysis, can be an indication of insufficient culture media flow or a consequence of the contraction of the hydrogel. Regarding the culture media flow rate of the ECs assays, it was possible to notice that in both designs of the chip the flow rate was not uniform during the time of the assays. It shows a peak in the first few days of operation and then gradually begins to decline. Besides, the automatic feeding system does not produce a constant media flow along the 24 h.

Although it was possible to demonstrate that the two developed chip designs are viable for long-term cell culture and that the optimized protocols are suitable for fibroblast growth, there is a need for further adaption and improvement of the protocols for assays with different ECs cultures for the generation of 3D human microvessel network.

Therefore, to optimize and increase the culture media flow rate in future works, some strategies may include: (i) increasing the width of media channels in both chip designs; (ii) increasing the level difference between reservoirs; (iii) increasing the pressure by using syringe pumps; (iv) shortening the time between flow direction

changes for 12 h and (v) increasing the thickness of the horizontal beams of the oscillatory feeding system for better support the reservoirs with the culture media.

Regarding the possible hydrogel contraction inside the tissue chambers, a preliminary test in wells may be necessary to observe the cells-hydrogel mixture interaction outside the chip and the use of an enzyme inhibitor such as aprotinin to the hydrogel mixture to inhibit fibrin degradation [50].

To promote ECs proliferation inside the chip, the addition of a purified protein such as CCBE1 into the culture media may be necessary to promote a highly vascular development since it has already contributed to develop a robust vessel network formation *in vivo* [25] and *in vitro* [49].

It is expected that after optimization of the protocols for ECs for achieving a viable microvessel network with HUVECs and fibroblasts cell co-cultures, further assays with other cell types will be conducted. Initially with CCBE1-deficient fibroblasts to confirm the highly vascular development of the CCBE1 protein in microfluidics and afterwards with iPS-derived endothelial cells, as originally planned.

The robustness and reproducibility of the chips, combined with the accessibility and versatility of the automatic oscillatory culture media delivery system, promise to make it a useful tool for the study of physiological and pathological mechanisms of CVDs and eventually a platform for vascular disease therapies.

6. References

[1] S. Kaptoge *et al.*, "World Health Organization cardiovascular disease risk charts: revised models to estimate risk in 21 global regions," *Lancet Glob. Heal.*, vol. 7, no. 10, pp. e1332–e1345, 2019, doi: 10.1016/S2214-109X(19)30318-3.

[2] Q. Ma, H. Ma, F. Xu, X. Wang, and W. Sun, "Microfluidics in cardiovascular disease research: state of the art and future outlook," *Microsystems Nanoeng.*, vol. 7, pp. 1–19, Mar. 2021, doi: 10.1038/s41378-021-00245-2.

[3] Q. Wu *et al.*, "Organ-on-a-chip: recent breakthroughs and future prospects," *Biomed. Eng. Online*, vol. 19, no. 1, pp. 1–19, 2020, doi: 10.1186/s12938-020-0752-0.

[4] R. Vitorino, S. Guedes, J. P. da Costa, and V. Kašička, "Microfluidics for Peptidomics, Proteomics, and Cell Analysis," *Nanomaterials*, vol. 11, no. 5, pp. 1–33, 2021, doi: 10.3390/nano11051118.

[5] A. Tajeddin and N. Mustafaoglu, "Design and Fabrication of Organ-on-Chips: Promises and Challenges," *Micromachines*, vol. 12, no. 1443, pp. 1–33, Nov. 2021, doi: 10.3390/MI12121443.

[6] F. Bragheri, R. M. Vázquez, and R. Osellame, "Microfluidics," in *Three-Dimensional Microfabrication Using Two-Photon Polymerization*, 2nd ed., T. Baldacchini, Ed. Elsevier Inc., 2020, pp. 493–526. doi: 10.1016/B978-0-12-817827-0.00057-6.

[7] J. S. Kwon and J. H. Oh, "Microfluidic Technology for Cell Manipulation," *Appl. Sci.*, vol. 8, no. 6, pp. 1–20, 2018, doi: 10.3390/app8060992.

[8] L. A. Low, C. Mummery, B. R. Berridge, C. P. Austin, and D. A. Tagle, "Organs-on-chips: into the next decade," *Nat. Rev. Drug Discov.*, vol. 20, no. 5, pp. 345–361, 2021, doi: 10.1038/s41573-020-0079-3.

[9] H. Jayamohan *et al.*, "Advances in Microfluidics and Lab-on-a-Chip Technologies," in *Molecular Diagnostics: Third Edition*, 3rd ed., G. P. Patrinos, Ed. Academic Press, 2017, pp. 197–217. doi: 10.1016/B978-0-12-802971-8.00011-0.

[10] A. G. Niculescu, C. Chircov, A. C. Bîrcă, and A. M. Grumezescu, "Fabrication and Applications of Microfluidic Devices: A Review," *Int. J. Mol. Sci.*, vol. 22, no. 4, pp. 1–26, 2021, doi: 10.3390/ijms22042011.

[11] A. Victor, J. Ribeiro, and F. F. Araújo, "Study of PDMS characterization and its applications in biomedicine: A review," *J. Mech. Eng. Biomech.*, vol. 4, no. 1, pp. 1–9, 2019, doi: 10.24243/jmeb/4.1.163.

[12] M. Wang and B. Duan, "Materials and Their Biomedical Applications," in *Encyclopedia of Biomedical Engineering*, vol. 1, R. Narayan, Ed. Elsevier Inc., 2019, pp. 135–152. doi: 10.1016/B978-0-12-801238-3.99860-X.

[13] C. Ma, Y. Peng, H. Li, and W. Chen, "Organ-on-a-Chip: A new paradigm for drug development," *Trends Pharmacol. Sci.*, vol. 42, no. 2, pp. 119–133, Feb. 2021, doi: 10.1016/J.TIPS.2020.11.009.

[14] G. A. Van Norman, "Limitations of Animal Studies for Predicting Toxicity in Clinical Trials: Is it Time to Rethink Our Current Approach?," *JACC Basic to Transl. Sci.*, vol. 4, no. 7, pp. 845–854, 2019, doi: 10.1016/j.jacbts.2019.10.008.

[15] Biotechnology Innovation Organization, Informa Pharma Intelligence, and Quantitative Life Sciences, "Clinical Development Success Rates and Contributing Factors 2011-2020," 2021.

[16] T. Osaki, V. Sivathanu, and R. D. Kamm, "Vascularized microfluidic organ-chips for drug screening, disease models and tissue engineering," *Curr. Opin. Biotechnol.*, vol. 52, pp. 116–123, 2018, doi: 10.1016/j.copbio.2018.03.011.

[17] A. Cochrane *et al.*, "Advanced in vitro models of vascular biology: Human induced pluripotent stem cells and organ-on-chip technology," *Adv. Drug Deliv. Rev.*, vol. 140, pp. 68–77, 2019, doi: 10.1016/j.addr.2018.06.007.

[18] A. Dellaquila, C. Le Bao, D. Letourneur, and T. Simon-Yarza, "In Vitro Strategies to Vascularize 3D Physiologically Relevant Models," *Adv. Sci.*, vol. 8, no. 19, 2021, doi: 10.1002/advs.202100798.

[19] A. M. A. O. Pollet and J. M. J. den Toonder, "Recapitulating the Vasculature Using Organ-on-Chip Technology," *Bioengineering*, vol. 7, no. 1, 2020, doi: 10.3390/bioengineering7010017.

[20] S. Jang, A. Collin de l'Hortet, and A. Soto-Gutierrez, "Induced Pluripotent Stem Cell-Derived Endothelial Cells: Overview, Current Advances, Applications, and Future Directions," *American Journal of Pathology*, vol. 189, no. 3. Elsevier Inc., pp. 502–512, Mar. 01, 2019. doi: 10.1016/j.ajpath.2018.12.004.

[21] A. Krüger-Genge, A. Blocki, R. P. Franke, and F. Jung, "Vascular Endothelial Cell Biology: An Update," *Int. J. Mol. Sci.*, vol. 20, no. 18, pp. 1–22, Sep. 2019, doi: 10.3390/ijms20184411.

[22] R. Xie, W. Zheng, L. Guan, Y. Ai, and Q. Liang, "Engineering of Hydrogel Materials with Perfusable Microchannels for Building Vascularized Tissues," *Small J.*, vol. 16, no. 15, pp. 1–17, 2020, doi: 10.1002/smll.201902838.

[23] F. Berthod, "Fibroblasts and Endothelial Cells: The Basic Angiogenic Unit," in *Angiogenesis: Insights from a Systematic Overview*, G. Santulli, Ed. Nova Science Publishers, 2013, pp. 145–157.

[24] N. G. Frangogiannis, "Fact and Fiction About Fibroblast to Endothelium Conversion: Semantics and Substance of Cellular Identity," *Circulation*, vol. 142, no. 17, pp. 1663–1666, Oct. 2020, doi: 10.1161/CIRCULATIONAHA.120.050875.

[25] F. Bonet, P. N. G. Pereira, O. Bover, S. Marques, J. M. Inácio, and J. A. Belo, "CCBE1 is Required for Coronary Vessel Development and Proper Coronary Artery Stem Formation in the Mouse Heart," *Dev. Dyn.*, vol. 247, no. 10, pp. 1135–1145, 2018, doi: 10.1002/dvdy.24670.

[26] Y. K. Kurokawa, R. T. Yin, M. R. Shang, V. S. Shirure, M. L. Moya, and S. C. George, "Human Induced Pluripotent Stem Cell-Derived Endothelial Cells for Three-Dimensional Microphysiological Systems," *Tissue Eng. Regen. Med. Int. Soc.*, vol. 23, no. 8, pp. 474–484, 2017, doi: 10.1089/ten.tec.2017.0133.

[27] S. Kim, H. Lee, M. Chung, and N. L. Jeon, "Engineering of functional, perfusable 3D microvascular networks on a chip," *R. Soc. Chem.*, vol. 13, no. 8, pp. 1489–1500, 2013, doi: 10.1039/c3lc41320a.

[28] Y. Zheng *et al.*, "In vitro microvessels for the study of angiogenesis and thrombosis," *Proc. Natl. Acad. Sci. U. S. A.*, vol. 109, no. 24, pp. 9342–9347, 2012, doi: 10.1073/pnas.1201240109.

[29] F. Shao *et al.*, "Microfluidic Encapsulation of Single Cells by Alginate Microgels Using a Trigger-Gellified Strategy," *Front. Bioeng. Biotechnol.*, vol. 8, p. 1181, Oct. 2020, doi: 10.3389/fbioe.2020.583065.

[30] M. L. Moya, Y. H. Hsu, A. P. Lee, C. W. H. Christopher, and S. C. George, "In Vitro Perfused Human Capillary Networks," *Tissue Eng. - Part C Methods*, vol. 19, no. 9, pp. 730–737, 2013, doi: 10.1089/ten.tec.2012.0430.

[31] M. Vila Cuenca *et al.*, "Engineered 3D vessel-on-chip using hiPSC-derived endothelial- and vascular smooth muscle cells," *Stem Cell Reports*, vol. 16, no. 9, pp. 2159–2168, Sep. 2021, doi: 10.1016/j.stemcr.2021.08.003.

[32] J. W. Weisel and R. I. Litvinov, "Fibrin Formation, Structure and Properties," in *SubCellular Biochemistry*, vol. 82, J. Robin Harris, Ed. 2017, pp. 405–456. doi: 10.1007/978-3-319-49674-0_13.

[33] A. Wnorowski, H. Yang, and J. C. Wu, "Progress, Obstacles, and Limitations in the Use of Stem Cells in Organ-on-a-Chip Models," *Adv. Drug Deliv. Rev.*, vol. 140, pp. 3–11, 2019, doi: 10.1016/j.addr.2018.06.001.

[34] K. Takahashi *et al.*, "Induction of Pluripotent Stem Cells from Adult Human Fibroblasts by Defined Factors," *Cell*, vol. 131, no. 5, pp. 861–872, 2007, doi: 10.1016/j.cell.2007.11.019.

[35] T. Mathur, J. J. Tronolone, and A. Jain, “Comparative Analysis of Blood-Derived Endothelial Cells for Designing Next-Generation Personalized Organ-on-Chips,” *J. Am. Heart Assoc.*, vol. 10, no. 22, p. 22795, Nov. 2021, doi: 10.1161/JAHA.121.022795.

[36] O. V Halaidych *et al.*, “Inflammatory Responses and Barrier Function of Endothelial Cells Derived from Human Induced Pluripotent Stem Cells,” *Stem Cell Reports*, vol. 10, no. 5, pp. 1642–1656, 2018, doi: 10.1016/j.stemcr.2018.03.012.

[37] A. Lin *et al.*, “Mural Cells: Potential Therapeutic Targets to Bridge Cardiovascular Disease and Neurodegeneration,” *Cells*, vol. 10, no. 3, pp. 1–25, 2021, doi: 10.3390/cells10030593.

[38] C. A. Hesh, Y. Qiu, and W. A. Lam, “Vascularized Microfluidics and the Blood-Endothelium Interface,” *Micromachines*, vol. 11, no. 1, pp. 1–27, 2020, doi: 10.3390/mi11010018.

[39] J. Nie *et al.*, “Vessel-on-a-chip with Hydrogel-based Microfluidics,” *Small*, vol. 14, no. 45, pp. 1–14, 2018, doi: 10.1002/smll.201802368.

[40] J. Ko, Y. Lee, S. Lee, S. R. Lee, and N. L. Jeon, “Human Ocular Angiogenesis-Inspired Vascular Models on an Injection-Molded Microfluidic Chip,” *Adv. Healthc. Mater.*, vol. 8, no. 15, pp. 1–10, 2019, doi: 10.1002/adhm.201900328.

[41] M. L. Moya, L. F. Alonzo, and S. C. George, “Microfluidic Device to Culture 3D In Vitro Human Capillary Networks,” *Methods Mol. Biol.*, vol. 1202, pp. 21–27, 2014, doi: 10.1007/7651-2013-36.

[42] E. Ferrari, F. Nebuloni, M. Rasponi, and P. Occhetta, “Photo and Soft Lithography for Organ-on-Chip Applications,” in *Methods in Molecular Biology*, 1st ed., vol. 2373, J. M. Walker, Ed. New York: Humana Press, 2022, pp. 1–19. doi: 10.1007/978-1-0716-1693-2_1.

[43] M. Magalhães, “Development of an in vitro platform for a 3D microphysiological systems of human iPS-derived endothelial cells,” NOVA School of Science and Technology, 2020.

[44] Terra Universal Inc., “FS209E and ISO Cleanroom Standards,” *Terra Univers.*, p. 4, 2012.

[45] Microchem, “SU-8 2000 Permanent Epoxy Negative Photoresist, Processing Guidelines for: SU-8 2025, SU-8 2035, SU-8 2050 and SU-8 2075.” pp. 1–5.

[46] A. K. Mora, S. Khan, B. S. Patro, and S. Nath, “Is DAPI assay of cellular nucleic acid reliable in the presence of protein aggregates?,” *Chem. Commun.*, vol. 56, no. 89, pp. 13844–13847, 2020, doi: 10.1039/d0cc04108d.

[47] J. Ryan, “Understanding and Managing Cell Culture Contamination,” *Corning Life Sci. Tech. Lit.*, pp. 1–24, 1994.

[48] K. Im, S. Mareninov, M. F. P. Diaz, and W. H. Yong, “An introduction to Performing Immunofluorescence Staining,” in *Methods in Molecular Biology*, vol. 1897, W. H. Yong, Ed. New York: Humana Press, 2019, pp. 299–311. doi: 10.1007/978-1-4939-8935-5_26.

[49] M. M. Silva *et al.*, “Full-length human CCBE1 production and purification: leveraging bioprocess development for high quality glycosylation attributes and functionality,” *J. Biotechnol.*, vol. 285, no. May, pp. 6–14, 2018, doi: 10.1016/j.jbiotec.2018.08.015.

[50] S. Mühleder *et al.*, “The role of fibrinolysis inhibition in engineered vascular networks derived from endothelial cells and adipose-derived stem cells,” *Stem Cell Res. Ther.*, vol. 9, no. 1, pp. 1–13, Feb. 2018, doi: 10.1186/s13287-017-0764-2.

[51] M. R. Green and J. Sambrook, “Estimation of Cell Number by Hemocytometry Counting,” *Cold Spring Harb. Protoc.*, vol. 2019, no. 11, pp. 732–734, 2019, doi: 10.1101/pdb.prot097980.

Annexe 1 – Microfabrication

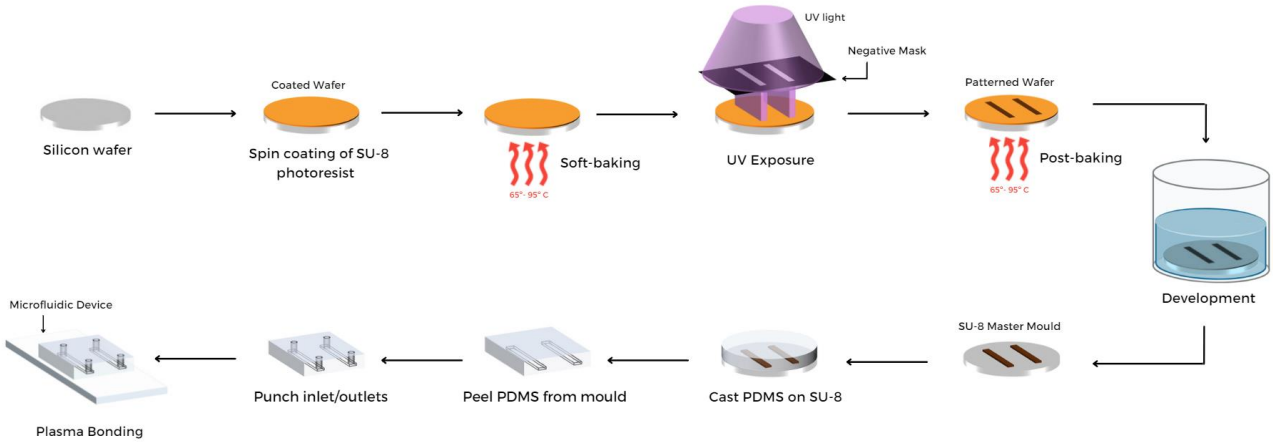

Figure I.1 – Schematic representation of photolithography and soft-lithography and sealing procedures for the fabrication of PDMS microfluidic devices (adapted from [42]).

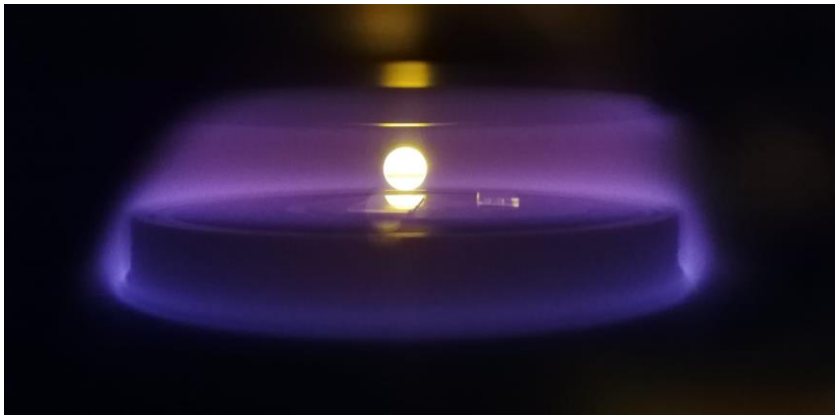

Figure I.2 – Purplish-blue colour plasma during the sealing process.

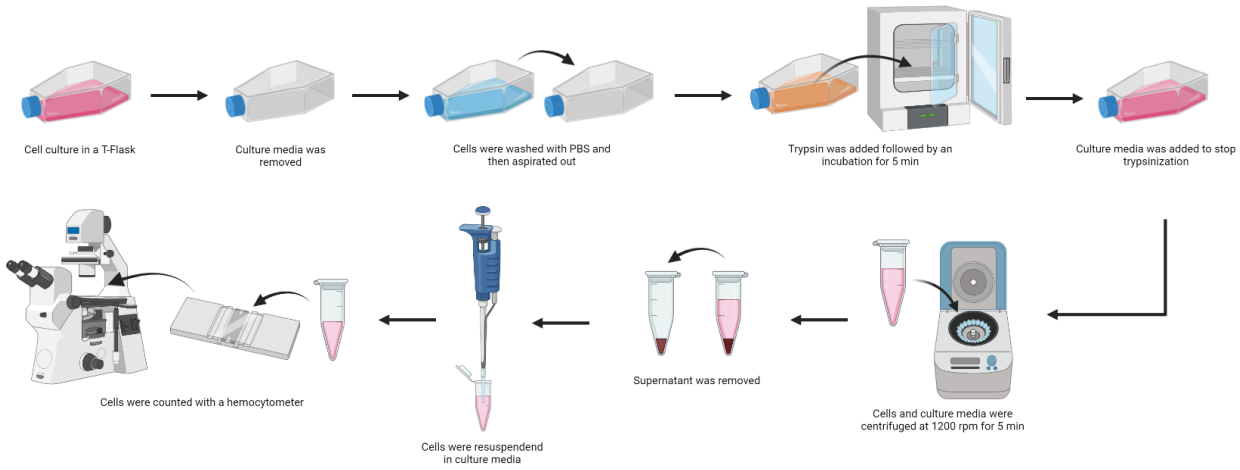

Figure II.1 – Schematic representation of cell passing, trypsinization and counting procedures [Figure created with Biorender.com].

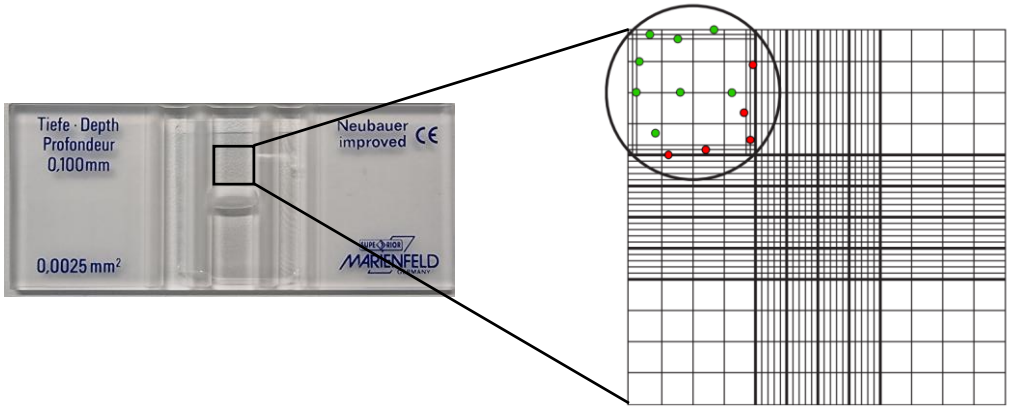

Figure II.2 – Hemocytometer with one chamber schematic for cell counting. Cells touching the middle line on the top and left are counted (green circles) and cells touching the middle line at the bottom and right (red circles) are not counted. The four corner squares of both chambers are counted although only one square and chamber are represented here (Adapted from [51]).

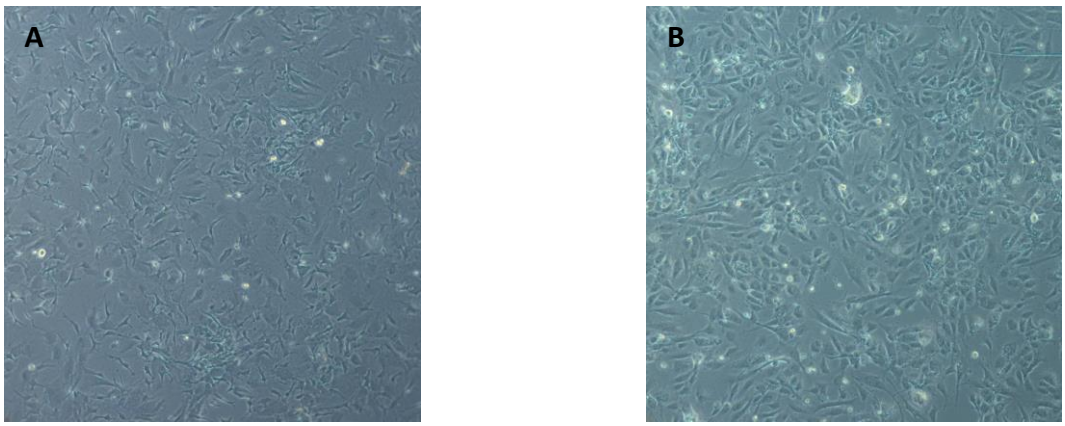

Figure II.3 – 90 % of confluency of (A) MEFs and (B) HUVECs (20x).

Annexe 3 – Experimental Assays

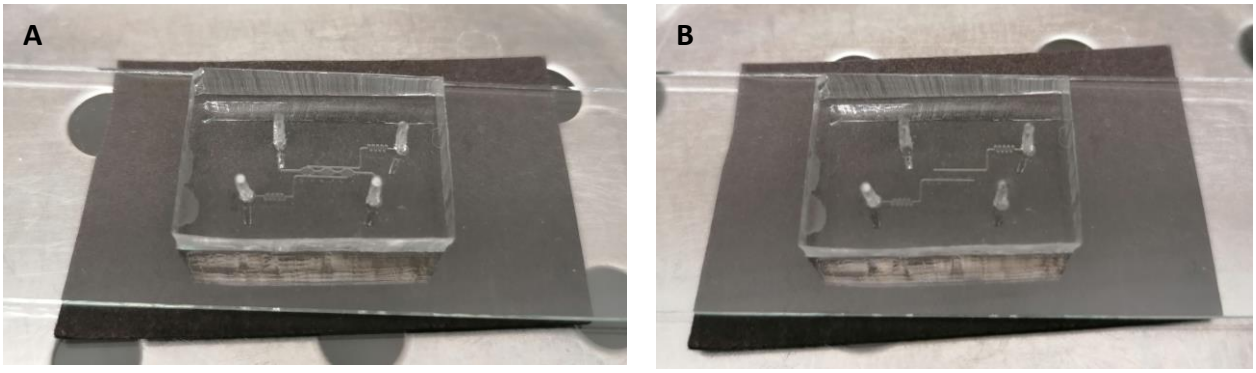

Figure III.1 – Filling process on top of a black surface. (A) Chip with empty chambers where it is possible to see the chambers; (B) The same chip after seeding the device where it is not possible to see the chambers.

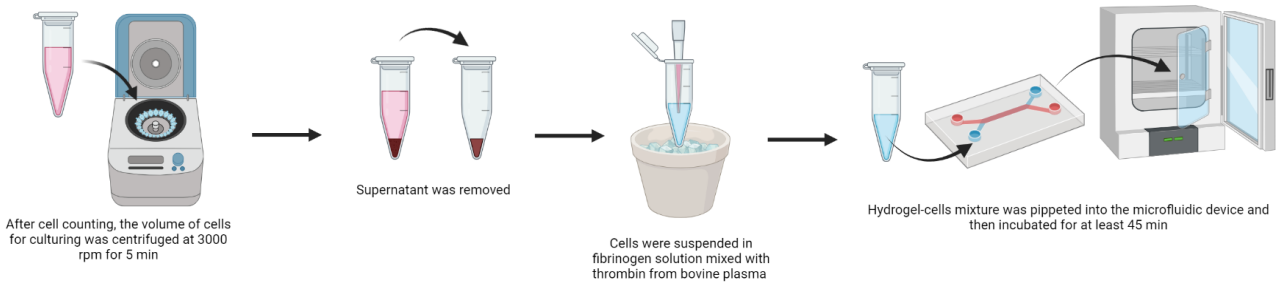

Figure III.2 – Schematic representation of the device seeding procedures [Figure created with Biorender.com].

Annexe 4 – Automatic Oscillatory Feeding System

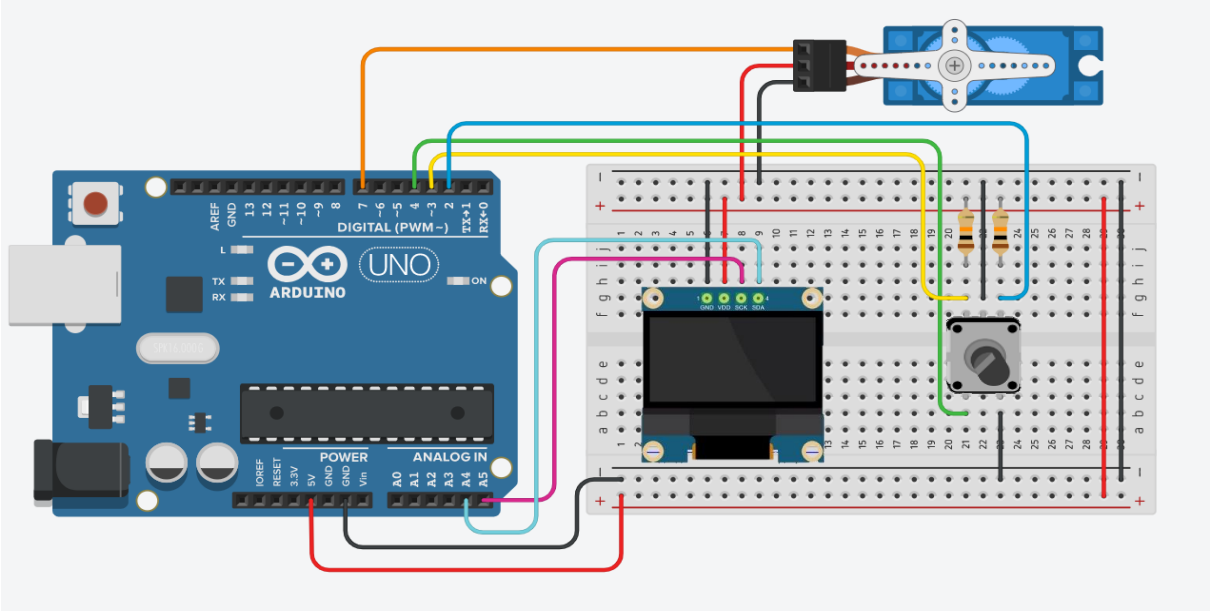

Figure IV.1 – Circuit design schematic [Figure created with AutoDesk Tinkercad Software].

```
//Libraries
#include <Servo.h>
#include <Wire.h>
#include <SPI.h>
#include <Adafruit_SH1106.h>
#include <Adafruit_GFX.h>

//OLED Inputs
#define OLED_ADDR   0x3C  //OLED i2c address
Adafruit_SH1106 display(-1);

#if (SH1106_LCDHEIGHT != 64)
#error("Height incorrect, please fix Adafruit_SH1106.h!");
#endif

//Rotary Encoder Inputs
#define encoderData   2            //Data pin connected to digital pin 2 (DT)
#define encoderClock  3            //Clock pin connected to digital pin 3 (CLK)
#define encoderButton 4            //Switch pin connected to digital pin 4 (SW)
volatile unsigned int encoder0Pos; //Encoder Position
unsigned int prev_encoder0Pos;     //Previous Encoder Position

//Servo Inputs
Servo myServo;

//Variables
byte valA = 0;              //Servo right angle valA<<valB
byte valB = 0;              //Servo left angle valB>>valA
unsigned int t;             //Waiting time (ms) between switching the servo angle
unsigned long system_time;  //Defines the time spent since the start of the program
unsigned long prev_time;    //Time recorded from system_time since the last servo's operation

byte menuCount = 1;         //Position of the arrow in the display menu
byte dir = 0;               //Direction of the servo
bool runState = false;      //Program does not run
bool side = false;          //Side is not defined
bool newPos = true;
bool display_angle = false; //Angle shown in the display
byte servo_state = 2;       //Atribute the side of the servo's angle
```

```
void setup() {
  myServo.attach (7);  //Servo connected to digital pin 7
  Serial.begin(9600);  //Serial Monitor setup

  //OLED setup
  display.begin(SH1106_SWITCHCAPVCC, OLED_ADDR);
  display.display();
  display.clearDisplay();
  attachInterrupt(0, doEncoder, CHANGE);  //Set an interrupt 0 on encoder pin, looking for a change signal
                                          //and executing the "doEncoder" Interrupt Service Routine (below)

  //Set encoder pins as inputs
  pinMode(encoderData, INPUT);
  digitalWrite(encoderData, HIGH);   // turn on pull-up resistor
  pinMode(encoderClock, INPUT);
  digitalWrite(encoderClock, HIGH);  // turn on pull-up resistor
  pinMode(encoderButton, INPUT);
  digitalWrite(encoderButton, HIGH); // turn on pull-up resistor
}

void loop() {
  byte clk = digitalRead(encoderButton);
  system_time = millis();
  menuCount = menuCheck(clk);
  encPosition();
  staticMenu();
  moveServo();
  display.clearDisplay();
  delay(50);
}

void staticMenu() {
  display.setTextSize(1);             //Define number of text
  display.setTextColor (WHITE);        //Define colour of text
  display.setCursor(50, 0);           //Position of the word MENU
  display.println("MENU");            //Write the word MENU

  display.setCursor(10, 10);          //Position of the word Right A:
  display.println("Min:");            //Write the word Right A:
  display.setCursor(60, 10);          //Position of the servo right angle
  display.println(valA);              //Write the servo right angle

  display.setCursor(10, 20);          //Position of the word Left A:
  display.println("Max:");            //Write the word Left A:
  display.setCursor(60, 20);          //Position of the servo left angle
  display.println(valB);              //Write the servo right angle

  display.setCursor(10, 30);          //Position of the word Time:
  display.println("Time:");           //Write the word Time:
  display.setCursor(60, 30);          //Position of the waiting time
  display.println(t);                 //Write the waiting time

  display.setCursor(10, 40);          //Position of the word Side:
  display.println("Side:");           //Write the word Side:
  display.setCursor(45, 40);          //Position of side options
  if (display_angle) {                //If the angle shown in the display is true
    display.println("Right");         //Write the word Right
  }
  else {                              //If the angle shown in the display is false
    display.println("Left");          //Write the word Left
  }

  display.setCursor(10, 50);          //Position of the word Start:
  display.println("Start:");          //Write the word Start:
  display.setCursor(50, 50);          //Position of the program's run options
  if (runState) {                     //If the program run
    display.println("ON");            //Write the word ON
  }
  else {                              //If the program does not run
    display.println("OFF");           //Write the word OFF
  }

  display.setCursor(2, (menuCount * 10));  //Position of the >
  display.println(">");                    //Write >
  display.display();
}
```

```
int menuCheck(byte clk) {
  if (clk == LOW && menuCount < 6) {
    menuCount++;
  }
  if (clk == LOW && menuCount >= 6) {
    menuCount = 1;
  }
  return menuCount;
}

void encPosition() {
  if (menuCount == 1) {
    if (prev_encoder0Pos != encoder0Pos) {
      valA = valA + (encoder0Pos - prev_encoder0Pos);
      prev_encoder0Pos = encoder0Pos;
    }
  }
  if (menuCount == 2) {
    if (prev_encoder0Pos != encoder0Pos) {
      valB = valB + (encoder0Pos - prev_encoder0Pos);
      prev_encoder0Pos = encoder0Pos;
    }
  }
  if (menuCount == 3) {
    if (prev_encoder0Pos != encoder0Pos) {
      t = (t + (encoder0Pos - prev_encoder0Pos));
      prev_encoder0Pos = encoder0Pos;
    }
  }
  if (menuCount == 4) {
    if (prev_encoder0Pos != encoder0Pos) {
      if (encoder0Pos > 5) {
        side = true;
        servo_state = 1;
        display_angle = true;
      }
      else {
        side = false;
        servo_state = 2;
        display_angle = false;
      }
      prev_encoder0Pos = encoder0Pos;
    }
  }
  if (menuCount == 5) {
    if (prev_encoder0Pos != encoder0Pos) {
      if (encoder0Pos > 5) {
        runState = true;
      }
      else {
        runState = false;
      }
      prev_encoder0Pos = encoder0Pos;
    }
  }
}
void doEncoder() {
  //If the Data state is high then the encoder is rotating counter clockwise
  if (digitalRead(encoderData) == HIGH) {
    if (digitalRead(encoderClock) == LOW && encoder0Pos > 0) {
      encoder0Pos = encoder0Pos - 1;   //Decrement the encoder's position count
      dir = 0;
    }
    else {  //Encoder is rotating clockwise
      encoder0Pos = encoder0Pos + 1;   //Increment the encoder's position count
      ++
      dir = 1;
    }
  }
  else {
    //If it's detect LOW signal in clock pin, button is pressed
    if (digitalRead(encoderClock) == LOW ) {
      encoder0Pos = encoder0Pos + 1;
      dir = 1;
    }
    else {
      if (encoder0Pos > 0) {
        encoder0Pos = encoder0Pos - 1;
        dir = 0;
      }
    }
  }
}
```

```
void moveServo () {
  byte i = 0;                             //Servo position
  if (runState == true) {                 //If the program run
    if (!side) {                          //If Side = false
      side = true;
      goto startvalB;                     //The program iniciates in startvalB
    }
    if (newPos) {
      for (i = 90; i >= valA; i -= 1) { //Servo moves from initial state to valA by decreasing 1 value
        myServo.write(i);
        delay(200);                       //The change of position takes 200 milliseconds
      }
      newPos = false;
    }
    if (((system_time - prev_time) > (t * 60 * 60 * 1000UL)) && servo_state == 1) {  //converting time in ms to h
      prev_time = system_time;
      for (i = valA; i <= valB; i += 1) { //Servo moves from valA to valB by increasing 1 value
        myServo.write(i);
        delay(100);                         //The change of position from valA to valB takes 100 milliseconds
      }
      servo_state = 2;
    }

startvalB:
    if (newPos) {
      for (i = 90; i <= valB; i += 1) { //Servo moves from the initial state to valB by increasing 1 value
        myServo.write(i);
        delay(200);                       //The change of position takes 200 milliseconds
      }
      newPos = false;
    }
    if ((system_time - prev_time > (t * 60 * 60 * 1000UL)) && servo_state == 2) {  //converting time in ms to h
      prev_time = system_time;
      for (i = valB; i >= valA; i -= 1) { //Servo moves from valB to valA by descreasing 1 value
        myServo.write(i);
        delay(100);                         //The change of position from valB to valA takes 100 milliseconds
      }
      servo_state = 1;
    }
  }
  else {
      prev_time = system_time;
  }
}
```

Figure IV.2 – Arduino Code used to control the automatic culture system.

SARA ISABEL GONÇALVES PRECATADO

OPTIMIZATION OF THE HUMAN IPS-DERIVED ENDOTHELIAL CHIP FOR DEVELOPMENT OF A 3D MICROPHYSIOLOGICAL VASCULAR CELLS SYSTEM

⟨2022⟩

NOVA SCHOOL OF SCIENCE & TECHNOLOGY